Annual Report

Hydrospheric Atmospheric Research Center (HyARC)

Nagoya University

2005

Annual Report

Hydrospheric Atmospheric Research Center (HyARC)

2005

NAGOYA UNIVERSITY

Contents

Foreword

Five years have passed since the establishment of the Hydrospheric Atmospheric Research Center (HyARC), Nagoya University, which aims to promote research on the global water cycle. The global water cycle is one of the primary components of the Earth system, and research into the global water cycle requires strong and wide collaboration among the science and application communities. HyARC functions as an inter-university collaborative system which may be unique in the world. During the last five years, the research style of HyARC has become clear, and specific projects and activities have been created and continued. These projects and activities include promotion of a follow-on project by the GEWEX Asian Monsoon Experiment (GAME), which was a sub-project under GEWEX and led by Prof. T. Yasunari of HyARC. Two projects are ongoing with the support of Core Research for Evolutional Science and Technology (CREST) in the Japan Science and Technology Corporation (JST). HyARC also has collaborations with the Institute of Humanity and Nature (RIHN), the National Institute of Information and Communication Technology (NICT), and others. HyARC has its own collaborative activities as well. We have selected a few Center Research projects to be funded from the HyARC budget. Although the amount of funding is limited, the projects are selected by HyARC with an eye to feasibility, necessity and collaboration requirements. This fiscal year we have three Center Research projects and nine workshops.

Even though the number of permanent staff at HyARC is limited to only eleven (four professors, four associated professors and three assistant professors), we have accepted many post-doctoral researchers who are highly active in research. We have also accepted graduate-school students in the Department of Environmental Studies. As part of contributions to the UNESCO International Hydrology Programme (IHP), we have conducted an IHP Training Course with funding for UNESCO from the Japan Trust in every Japanese fiscal year. This year's, theme was "Water and Carbon Cycles in Terrestrial Ecosystems".

Nagoya University has undergone a major change, and its management system has become more flexible, with accountability becoming much more important. At the same time, not only is accountability being emphasized, but research publications and other outreaches are also being encouraged.

UYEDA Hiroshi
Director
Hydrospheric Atmospheric Research Center

Staff and Organization

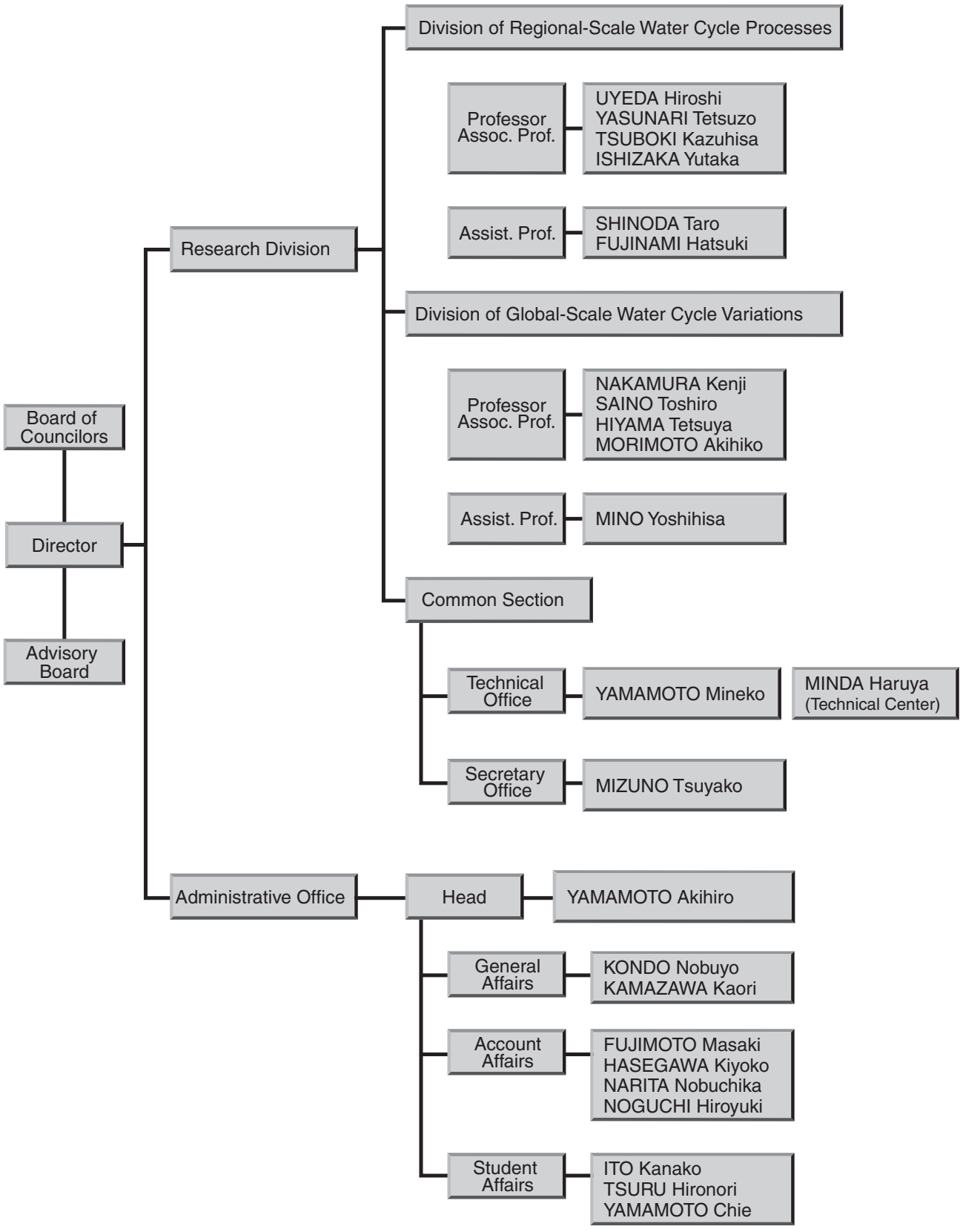

Administration

Board of Councilors

UYEDA Hiroshi: *Director, Prof., Hydrospheric Atmospheric Research Center*
YASUNARI Tetsuzo: *Prof., Hydrospheric Atmospheric Research Center*
NAKAMURA Kenji: *Prof., Hydrospheric Atmospheric Research Center*
SAINO Toshiro: *Prof., Hydrospheric Atmospheric Research Center*
UEMURA Daisuke: *Prof., Graduate School of Science*
HARAGUCHI Hiroki: *Prof., Graduate School of Engineering*
HATTORI Shigeaki: *Prof., Graduate School of Bioagricultural Sciences*
KANZAWA Hiroshi: *Prof., Graduate School of Enviromentral Studies*
FUJII Ryoichi: *Prof., Solar-Terrestrial Environment Laboratory*

Advisory Board

●Members from Nagoya Unisversity
UYEDA Hiroshi: *Director, Prof., Hydrospheric Atmosphric Research Center*
YASUNARI Tetsuzo: *Prof., Hydrospheric Atmospheric Research Center*
NAKAMURA Kenji: *Prof., Hydrospheric Atmosphric Research Center*
SAINO Toshiro: *Prof., Hydrospheric Atmosphric Research Center*
ISHIZAKA Yutaka: *Assoc. Prof., Hydrospheric Atmosphric Research Center*
TSUBOKI Kazuhisa: *Assoc. Prof., Hydrospheric Atmosphric Research Center*
HIYAMA Tetsuya: *Assoc. Prof., Hydrospheric Atmosphric Research Center*
MORIMOTO Akihiko: *Assoc. Prof., Hydrospheric Atmosphric Research Center*
TSUJIMOTO Tetsuro: *Prof., Graduate School of Engineering*
OHTA Takeshi: *Prof., Graduate School of Bioagricultural Sciences*
AGETA Yutaka: *Prof., Graduate School of Environment Studies*
MATSUMI Yutaka: *Prof., Solar-Terrestrial Environment Laboratory*
●Members outside Nagoya University
FUJIYOSHI Yasushi: *Prof., Institute of Low Temparature Science, Hokkaido University*
HANAWA Kimio: *Prof., Graduate School of Science, Tohoku University*
SUMI Akimasa: *Prof., Center for Climate System Research, The University of Tokyo*
FUKUSHIMA Yoshihiro: *Prof., Research Intutite for Humanity and Nature*
YAMANAKA Manabu: *Prof., Graduate School of Science and Technology, Kobe University*

High Resolution Modeling of Atmospheric Water Circulation Systems Using a Cloud-Resolving Model

The purpose of this research is the explicit simulation of clouds and organized precipitation systems using the cloud-resolving model in a large domain and very fine grid (less than 1 km). In this research, we utilized the Cloud Resolving Storm Simulator (CReSS), which is a cloud-resolving model developed for parallel computers. Using CReSS on the Earth Simulator, we performed simulation experiments of important cloud and precipitation systems. We performed simulation experiments of the Niigata-Fukushima heavy rainfall event that occurred in July 2004. The investigation of the heavy rainfall event shows that an intense rainband forms and is maintained within the subsynoptic-scale low along the Baiu front (Figs. 1 and 2). Simulations of snow storms over the Sea of Japan were also performed as well as those over the Great Lakes region of Canada. Snowstorm experiments show various types of precipitation systems are composed of intense convective clouds in cold air streams (JPCZ). Figure 3 shows the simulated convergence zone over the Sea of Japan. Transversal cloud bands extend along the vertical wind shear to the northeast of the wide convective cloud band (the rectangle in the figure) while longitudinal cloud bands develop on the southwest side. Investigation of typhoons is also an important objective of this research. They develop owing to the close interaction between large-scale motion and cumulonimbus convections.

Figure 4 shows a 3-dimensional display of the simulated clouds of Typhoon 0418. The horizontal resolution is 1 km. The simulation shows very realistic features of the typhoon and individual clouds. These experiments revealed both the very detailed structure of individual precipitation clouds as well as the overall structures of large-scale systems.

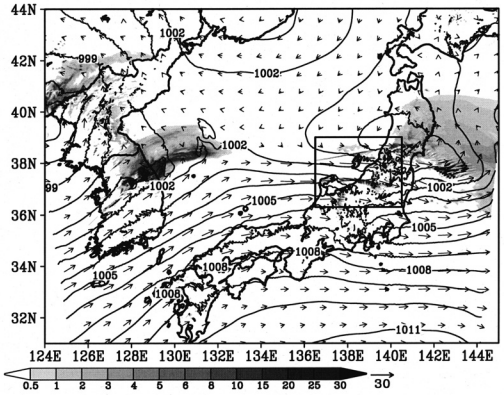

Fig. 1 Surface pressure (contour lines; hPa) and rainfall intensity (gray levels; mm^{-1} and horizontal velocity (arrows) at a height of 1610 m at 0020 UTC, July 13, 2004. The rectangle indicates the region of Fig. 2.

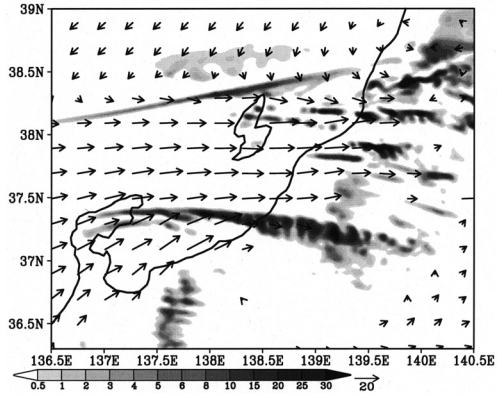

Fig. 2 Same as Fig. 1 but for the region of the rectangle in Fig. 1 and at a height of 436 m.

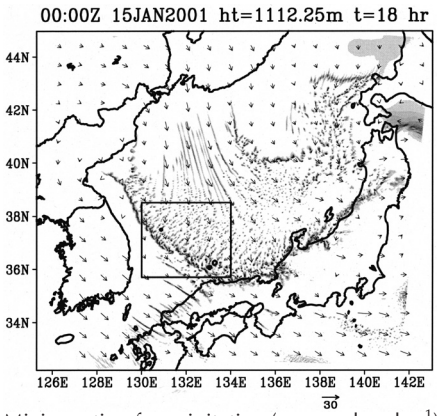

Fig. 3 Mixing ratio of precipitation (gray scale; $g\,kg^{-1}$) and horizontal velocity (arrows) at a height of 1.1 km.

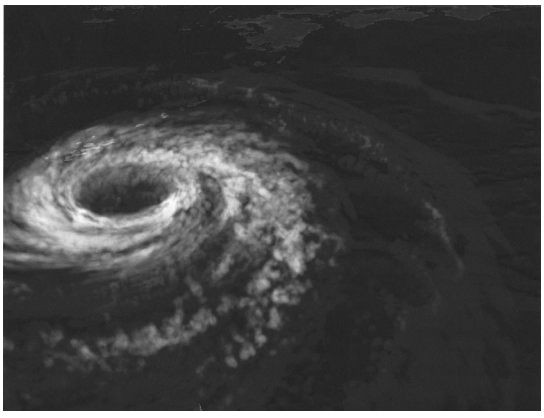

Fig. 4 Three-dimensional display of clouds simulated for Typhoon 0418 using POV-Ray (courtesy of Professor T. Aoki, Tokyo Institute of Technology).

Application of stable isotopes of water for evaluation of multi-scale water cycle processes

Stable isotope ratios of water (δD & δ^{18}O) and those anomalies from well-known meteoric water line (d-excess = δD-8 · δ^{18}O) are good indicators to identify origins of precipitation water, river water, groundwater, and the like. Since isotope ratios of water are controlled by kinetic or equilibrium fractionation processes in evaporation or condensation, the ratios are applicable for evaluations of global water cycles as supporting tools for water balance calculation, paleo-climate variation, and basin-scale hydrological studies.

HyARC is conducting mass spectral analyses of stable isotope ratios of water as one of the HyARC Research Programs. In fiscal 2005, we comprehensively analyzed 2,379 water samples upon request from 8 domestic researchers.

We applied for a research grant to the Japan Society for the Promotion of Science (JSPS) and were successful in gaining acceptance of our research plan named, "Comprehensive Study on Meso-Scale Precipitation System with Use of Stable Isotope Ratios of Water" from fiscal 2005 through 2007. We are also proposing several other methodologies to evaluate multi-scale water cycles in the hydrological processes of evapotranspiration, atmospheric boundary-layer process, cloud development, and precipitation processes. Our current targets are:

- Use of stable isotope ratios of water to understand the mechanism of meso-scale water cycle systems in coordination with other precise meteorological measurements (e.g., multi-band radars, radio-soundings, and rain drop size measurements) together with objective re-analyzed data sets, and
- Use of stable isotope ratios of water to model multi-scale water cycle processes.

This research plan also aims to promote studies in isotope hydrology and to link activities from the multi-scale point of view in water cycles among several research groups in Japan. We are conducting annual science workshops related to this research plan. In fiscal 2005, we held a workshop from February 21 to 22, 2006. A total of 36 participants attended the workshop, and valuable discussions were held on the issues described above.

Observational study on the characteristics of clouds/precipitation, atmospheric boundary layer, and ocean surface around the Okinawa Island

The Okinawa Islands are located in the southwest of Japan, and are surrounded by warm ocean bearing the Kuroshio Current. This area is known as a typhoon route. There the National Institute of Information and Communications Technology (NICT) established excellent observational sites with microwave remote sensing instruments, including of: meteorological radar, windprofilers, ocean radar, and other ground observation systems. Using these instruments, the characteristics of the atmosphere and ocean around the Okinawa Islands are to be studied.

In June 2005, a kick-off symposium was held on this topic at the headquarters of the NICT in Koganei, Tokyo, where many expectations held for this project were presented. In March 2006, a workshop on this topic was held at Nagoya University. Precipitation system studies, including precipitation particle characteristics estimated from a full-polarization Doppler radar, were presented. Results for mixed-layer evolution using Doppler radar and windprofilers and for ocean current using ocean radar were also presented. The study was conducted as a collaboration between HyARC and the NICT.

21st Century COE Program, Dynamics of the Sub-Earth-Life Interactive System

Two years have passed since the beginning of the 21st Century COE Program, Dynamics of the Sub-Earth-Life Interactive System, and in May 2005, we received our interim evaluation. This COE program consists of core member faculty (4 from our center), associate member faculty, postdoctoral researchers and DC researchers (doctoral course students hired as research assistants) who take part in various activities. At every level of our staff, in all their respective fields, there is much enthusiasm and critical insights for overcoming the barriers that heavily subdivide the fields of Earth science. Young faculty and postdoctoral scientists have played a central role in arranging Crosscutting Research Seminars which have already been held more than 30 times, and other research workshops focusing on crosscutting themes. These efforts have lead to the emergence of collaborative research that reach beyond departmental and organizational boundaries.

Unlike traditional academic societies, the Crosscutting Research Program and poster sessions for DC researchers provide a unique opportunity for young scientists to break out of their own particular narrow field of study and comment upon each other's work to gain a broader perspective of their current studies. There remains debate on whether it is not better for graduate students seeking PhDs to focus on their particular studies rather than diverting their efforts in such activities. However, the opportunity to gain a wide and long-term viewpoint and insight into the earth system is also important. This philosophy is in harmony with the mission of our center for training future researchers of the hydrological and climatological aspects of the earth system. The Crosscutting Research Program which targets DC researchers as well, provides an ideal opportunity for postdoctoral researchers and graduate students for such training.

On the educational front, we have initiated lectures on COE Earth Science as a special course in the graduate school of environmental studies. This course combines cutting edge lectures by faculty members with discussions and discourse with the graduate students. In the 2005 school year, we started to provide this class as a regular course.

First held in 2004, we continued in hosting a public open seminar in the Nagoya city science museum. In the following year, keeping in the spirit of the world expo held in Aichi Prefecture, we held a seminar in July entitled, "Ice age to global warming and future — Let's think about the environmental change in Asia and impact of human activities" (http://www.coe.env.nagoya-u.ac.jp/meeting/domestic/fyh17/poster.pdf) to great success. In the following December, the COE co-hosted with the HyArc center a symposium entitled, "Does vegetation change climate? — Climate and vegetation changes through hydrological cycles" in the Nagoya University Symposion hall in November. We invited Prof. Shukuro Manabe of Princeton university, a pioneer and leader in climate modeling, for a public seminar entitled "Water resource changes due to global warming" and held a three day international symposium entitled, "Global warming in the ice age climate". This symposium attracted many visitors from around Japan and was very fruitful.

In the past two and a half years, in addition to many articles accepted to various international journals, three articles were accepted in the journal, *Nature*, and one article was accepted in the journal, *Science*, which includes collaborative research.

Core Research for Evolutional Science and Technology (CREST)

● Lower Atmosphere and Precipitation Study (LAPS)

The Lower Atmosphere and Precipitation Study (LAPS) is one of the projects conducted in the Core Research for Evolutional Science and Technology (CREST) of the Japan Science and Technology Agency (JST). The CREST projects all have strategic research themes (http://www.jst.go.jp/kisoken/en). LAPS is under the theme of "R&D of Hydrological Modeling and Water Resources Systems" supervised by Prof. K. Musiake of Fukushima University. The objective of LAPS is to clarify the relationship between the planetary boundary layer (PBL) and the precipitation system.

The field experiment in China was extended to cover the transition from dry season to wet season so that two data sets for transition periods were obtained. The observation in China concluded in autumn of 2005, and the instruments were removed and transported to Japan. Another field experiment was conducted on the Okinawa main island for about two weeks in July. A polarimetric Doppler radar which can observe strong turbulences in the PBL is operated there by the National Institute of Information and Communications Technology. Using the radar, data on PBL structure including that for weak rain was obtained.

Notable progress was made in the model study. The model simulates large eddies in the PBL. The model parameters were first tuned to reproduce the observational data, such as PBL evolution and surface fluxes. Using the model results, vertical profiles of the heat and water vapor were estimated.

Solution Oriented Research for Science and Technology (SORST)

● Satellite Monitoring of Ocean Primary Productivity

The ocean is the largest reservoir of water and carbon dioxide on the Earth's surface, and so the air-sea exchange of water and carbon dioxide plays central role in determining the climate system of the Earth. The air-sea exchange of heat (water) and carbon dioxide is affected by phytoplankton because they determine optical properties of the near-surface layers of the ocean and absorb carbon dioxide by primary productivity. To better predict climate variability, quantitative knowledge of the abundance and productivity of phytoplankton on a global scale is required for a mechanistic understanding of their regulating processes, thereby helping to improve climate prediction models. In practical terms, this knowledge and understanding can be obtained only by satellite observations, but because of the difficulty in obtaining in situ data for validation, those satellites data are yet to be fully exploited.

To overcome this difficulty, we have been working on developing an in situ monitoring system for ocean primary productivity to validate primary productivity data from satelittes. The system, composed of an underwater winch system with a profiler buoy equipped with a fast repetition-rate fluorometer, was successfully developed with the support of Core Research for Evolutional Science and Technology from the Japan Science and Technology Agency. Following this, a continuation project entitled "Satellite Monitoring of Ocean Primary Productivity (SMOPP)" was approved by the JST within the framework of the Solution Oriented Research in Science and Technology Program. The goal of the SMOPP project is to design an operational monitoring system for ocean primary productivity on a global scale. To attain this goal, we are to conduct routine operation of the monitoring system and obtain validated time-series satellite data on primary productivity, to be utilized in combination with other time-series satellite data on physical-forcing parameters on the ocean surface, for process studies on the response of ocean biology to atmospheric forcing to the ocean.

In fiscal 2005, our efforts included 1) test operation of an underwater winch system, 2) improvement of the winch system and a profiler buoy, 3) improvement of afast repetition-rate fluorometer, 4) development and validation of a primary productivity algorithm, and 5) process study on the response of ocean biology to atmospheric forcing. These efforts were conducted in collaboration with Tokyo University of Marine Science and Technology and the Nichiyu Giken Co., Ltd. (for 1 and 2), Tokai University and Kimoto Electric Co., Ltd. (for 3), Nagasaki University, Hokkaido University, TUMST, University of Tokyo, Fisheries University, Rutgers University, Chulalongkorn University, and Kasetsart University (for 4), and the Japan Agency for Marine-Earth Science and Technology and its Frontier Research Center for Global Change (for 5).

Because the ultimate goal of the SMOPP project is to propose an operational ocean observation system, emphasis is placed on having a wide international acquaintance. In fiscal 2005, presentations were given at the PICES-CLIVAR meeting in Seoul, the TOS meeting in Paris, a seminar at the National Oceanography Center, Southampton, the ICDC7 meeting in Colorado, the PICES meeting in Vladivostok, and the CLIVAR workshop and PICES CC-S meeting in Hayama.

Laboratory of Meteorology

Daily weather simulation around the Japanese Islands by using the CReSS

Our laboratory has performed daily high-resolution weather simulations around the Japanese Islands by using the CReSS (Cloud Resolving Storm Simulator) since December 2004. During this simulation period, we have accumulated continuous distributions of pressure, wind, precipitation and other meteorological parameters from the simulation, except for the times when the simulation was interrupted. These simulation results are presented on the web-site of our laboratory (http://www.rain.hyarc.nagoya-u.ac.jp/CReSS/fcst_exp.html). We utilize the JMA-RSM (Japan Meteorological Agency-Regional Spectral Model) data distributed by the Japan Meteorological Business Support Center as the initial and boundary conditions of these simulations. We performed daily weather simulations with a 5-km horizontal grid resolution after the RSM data was renewed.

We present the results of the daily weather simulation of the snowfall event in the Central Japan Region on February 1 to 2, 2005. Figure 1 shows the distribution of the precipitation obtained by the JMA radar. A snow cloud band intrudes from the Sea of Japan to the Nagoya area. There was a heavy snowfall event in Nagoya City on this day. The daily weather simulation results represent these snow cloud bands well. We utilized the daily weather simulation results in order to determine plans of aircraft observation across the Baiu front over the East China Sea in June 2005. Thus, the daily weather simulation is proved to be qualitatively in good agreement with the weather phenomena.

We will continue the daily weather simulation by using the CReSS and the analysis of these results statistically in order to improve the CReSS, especially its parameterization schemes. We also intend to improve the cumulus and saturation adjustment parameterizations in the GCM (General Circulation Model) by analyzing the accumulated daily weather simulation results statistically. We propose to contribute to disaster prevention by utilizing daily weather simulations with a 1-km grid resolution.

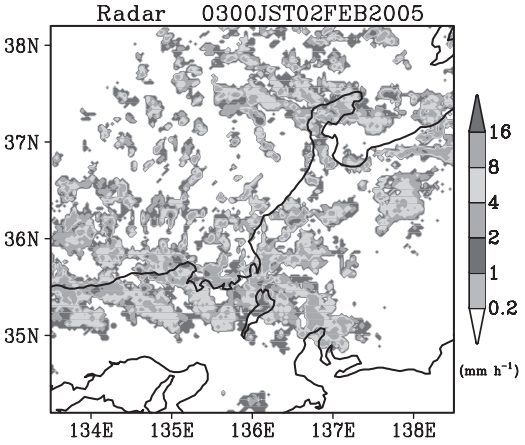

Fig. 1 Horizontal distribution of precipitation rates observed by JMA radar at 03 JST (9 hours ahead of UTC) on February 2, 2005.

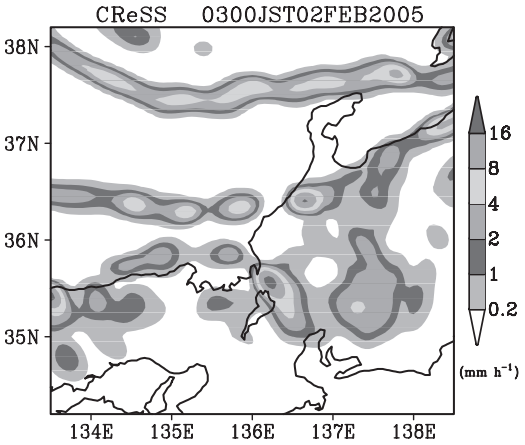

Fig. 2 Same as Fig. 1 but for the daily weather simulation results by the CReSS at the same time.

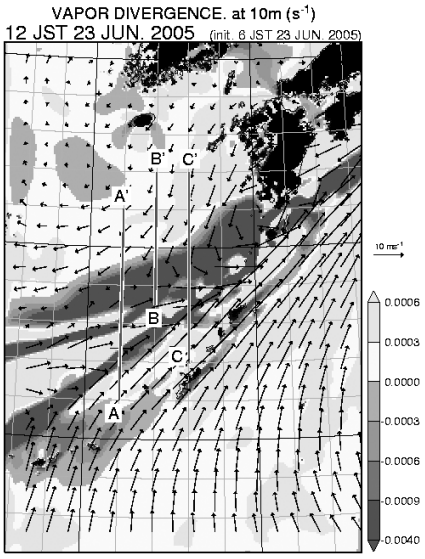

Fig. 3 Horizontal distribution of convergence of water vapor (shaded) and horizontal wind field (vector) at a height of 10 m (around the surface) over the East China Sea at 12 JST on June 23, 2005. The aircraft observation was carried out along the prescribed line A-A′ across the convergence zone of water vapor.

Quantitative prediction of heavy rainfall caused by Typhoon 0423

When a typhoon is positioned over the low-latitude ocean, it is composed of active cumulonimbus clouds. The eye-wall and spiral rainbands are conspicuous within the typhoon. On the other hand, they are often modified and become indistinct when the typhoon moves to the mid-latitudes around the Japanese Islands or the Korean Peninsula. Although the latent heat from the sea is reduced, a heavy rainfall occasionally occurs over the land resulting in floods and landslides. One significant case of heavy rainfall caused by typhoons in the mid-latitude occurred in the central part of Japan on October 20, 2004. Typhoon 0423 brought heavy rainfall and caused a severe disaster due to flooding. Even though the eye-wall and spiral rainbands were indistinct when T0423 approached the area, intense rainfall of more than 30 mm hr^{-1} hit the area. We studied the heavy rainfall associated with T0423 using the cloud-resolving model. The purpose of the present study is to clarify the formation process of heavy rainfall caused by the typhoon when it reached the mid-latitudes.

In order to conduct simulation and numerical experiments of high-impact weather systems, we have been developing the Cloud Resolving Storm Simulator (CReSS), a cloud-resolving numerical model which is a non-hydrostatic and compressible equation model using detailed cloud microphysics. In order to simulate both the overall structure of T0423 and the detailed structure of the heavy rainfall, the calculation domain is as large as 1536 times 1408 km in the horizontal with a horizontal resolution as high as 1 km. We performed a 30-hour simulation of T0423 from 1200UTC, October, 19, 2004.

The initial and boundary conditions were provided by the JMA-RSM (Japan Meteorological Agency-Regional Spectral Model) output.

The results of the prediction experiment show that the typhoon-track, total rain distribution (Fig. 4) and rainfall intensity were quantitatively simulated. The heavy rainfall in the northern Kinki District was simulated successfully (Fig. 5). This was associated with the intrusion of the intense upper-level rainband. The precipitation predictions by CReSS were compared with JMA surface observations and their accuracy was evaluated statistically using parameters of root mean square error, correlation coefficient, threat score, and bias score. Evaluation of the prediction experiment using these parameters shows that the CReSS model simulated the heavy rain with sufficiently high scores during the period of the prediction experiment. The successful results indicate that the cloud-resolving model is useful and effective for the accurate and quantitative prediction of heavy rainfall.

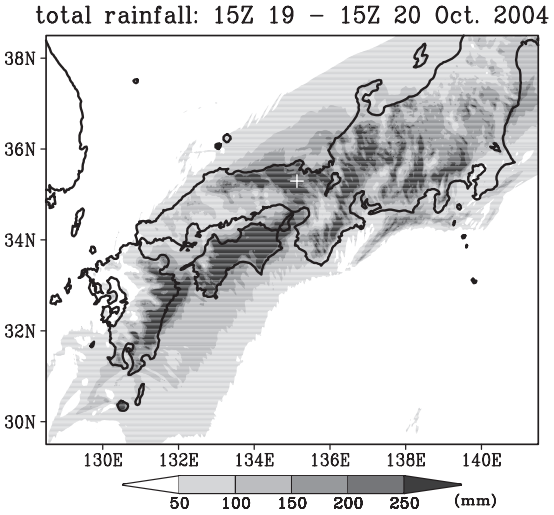

Fig. 4 Total rainfall (mm) obtained from the prediction experiment using the CReSS model for the period from 15 UTC, 19 to 15 UTC, October 20, 2004. The cross in the figure indicates Fukuchiyama.

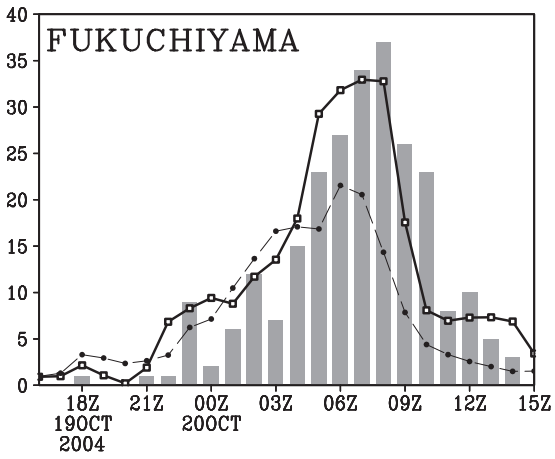

Fig. 5 Time series of rainfall rates (mm hr^{-1}) of AMeDAS observation (bars), predictions by CReSS (solid line) and RSM (dashed line) at Fukuchiyama in the northern Kinki District.

Heavy rainfall to the south of the Baiu front

In East Asia, heavy rain is often caused in association with the Baiu/Meiyu front. Understanding and numerical prediction of the heavy rains are one of the most important objectives of mesoscale meteorology. Since intense convective systems are usually composed of cumulonimbus clouds, a cloud resolving numerical model is necessary for simulation of heavy rain. In order to perform simulations and numerical experiments of cloud and precipitation systems, we have been developing a cloud-resolving numerical model named the Cloud Resolving Storm Simulator (CReSS).

Since heavy rainfall systems often have a multi-scale structure ranging from the cloud-scale to the synoptic-scale, a large computational domain and a very high-resolution grid to distinguish individual classes of the multi-scale structure are necessary to simulate the evolution of convective systems. The purpose of this research is the simulation of a localized heavy rain which occurred to the south of the Baiu front. Using the results of the simulation, we studied the complex processes of the heavy rainfall.

The heavy rain event occurred July 19–20, 2003 in Kyushu, which is in western Japan. During this period, the Baiu front was located to the north of Kyushu. The most intense rain occurred during the period of 16–22 UTC, July 20. The total amount of rain of this period reached about 210 mm at Minamata City which is located in western Kyushu. The heavy rain caused a flood and 21 people were killed. Radar data provided by JMA (the Japan Meteorological Agency) show that intense echo systems developed within a mesoscale convective system and moved into the west coast of Kyushu. An intense rainband extended in the east-west direction and some orographic rainfall echoes developed in western Kyushu.

The initial time of the simulation experiment with a horizontal resolution of 1 km was 00 UTC, July 19, 2003, and 24-hour integration was performed. The experiment successfully simulated the localized heavy rain. The rainfall pattern in the simulation is quite similar to the observation data in regard to the pattern and intensity of rain. The results showed that an intense rainband developed to the west of Kyushu in association with the cloud cluster. The simulation also shows that another rainband is present to the south of the main rainband. It forms on the lee side of the small Koshiki islands over the sea (Fig. 6). If the small islands are removed in a sensitivity experiment, the rainband completely disappeared (Fig. 7). This indicates that the islands are essential for the formation of the rainband. We consider that both of the two rainbands caused the localized heavy rainfall.

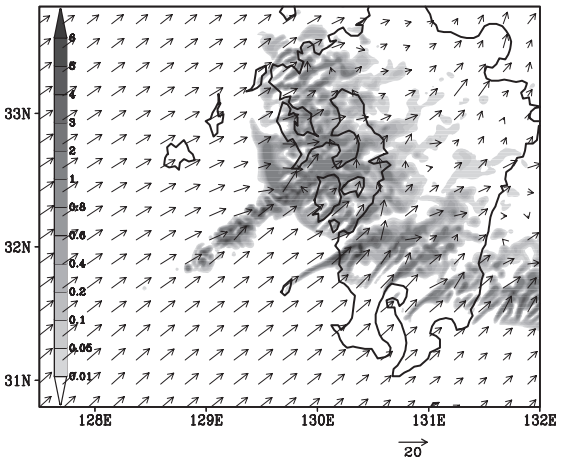

Fig. 6 Simulation experiment of the Minamata heavy rainfall event on July 19, 2003. Cloud and rain mixing ratio (g kg^{-1}) and horizontal velocity at a height of 1500 m at 15 hours from the initial time.

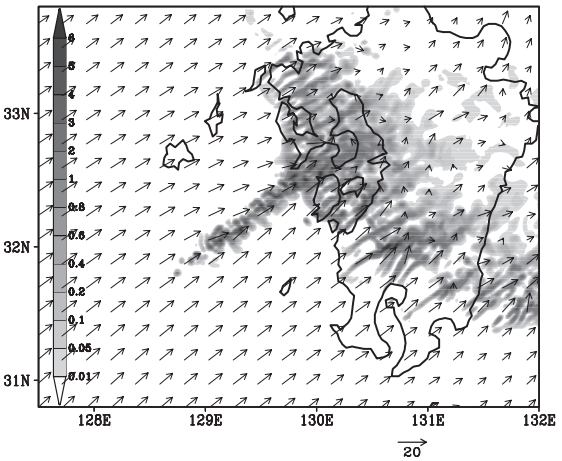

Fig. 7 Same as Fig. 6 but for the sensitivity experiment without the Koshiki islands.

Time variation of cumulonimbus clouds and precipitable water vapor over a slope of mountains with a valley wind in summer

In summer, cumulonimbus clouds develop over the slope of mountains with a valley wind and often bring heavy rainfall to surface. The cumulonimbus clouds are one of the dominant elements of the water circulation process associated with the valley wind circulation. In this study, to investigate the role of cumulonimbus clouds in the water circulation process associated to the valley wind circulation, the evolution of cumulonimbus clouds which developed over the slope of mountains with a valley wind and the time variation of precipitable water vapor over the slope was examined. The mountains chosen as an example include the Ryoupaku Mountains and the Hida Highland to the north of the Noubi Plain.

The radar data of Japan Meteorological Agency (JMA), AMeDAS data of JMA and precipitable water vapor (PWV) retrieved from dense network of global positioning system (GPS) operated by Geographical Survey Institute (GSI) of Japan were utilized. The case was on July 4, 2000, when a high at surface was present over Japan and a cold and dry air covered over Japan. Local Standard Time (LST = UTC + 9 hours) is used in this paper.

Figure 8 shows the convective echo observed by JMA radar which correlates with a cumulonimbus cloud and the wind speed and direction at each AMeDAS point. At 1230 LST, the convective echo P1 developed over the peak of the mountains with a valley wind (Fig. 8a). At 1410 LST, the outflow from the weakened echo P1 extended over the peak (Fig. 8b). On the southern and northern slopes of the mountains, convective echoes N1 and H1 developed. Echo N1 notably had a rainfall intensity of over 64 mm h^{-1}. At the Hachiman of AMeDAS observation point, a rainfall of 14 mm in 60 minutes and outflow from the convective echo N1 were observed when it passed. Valley wind blew on the downslope side of echo N1. At 1530 LST, the convective echo N2, which had a rainfall intensity over 64 mm h^{-1}, developed on the downslope side of the weakened echo N1 (Fig. 8c). At the peak of mountains, namely the upslope side of the echo N1, the convective echo P2 appeared.

Figure 9 shows the time deviation of PWV and the wind speed and direction at each AMeDAS point. At 1230 LST, PWV increased over the peak of the mountains with the development of the convective echo P1 (Fig. 9a). At the foot and on the slope of mountains with valley wind, PWV increase only a little or decreased. At 1410 LST, PWV decreased abruptly with the weakened echo P1 (Fig. 9b). On the slope, PWV increased abruptly with the development of echo N1. PWV also increased on the downslope side of echo N1 where valley wind blew. At 1530 LST, PWV decreased at the weakened echo N1 (Fig. 9c). A large gradient of time deviation of PWV existed for echo N2. Over the peak of mountains, PWV increased with the appearance of the echo P2.

After the cumulonimbus cloud caused by the transportation of water vapor to the peak of mountains by valley wind, a new cumulonimbus cloud occurred over the slope where the outflow from the old cumulonimbus cloud and the valley wind made horizontal convergence and PWV increased. The cumulonimbus cloud developed in the region where PWV increased abruptly and had a large rainfall intensity. It is considered that the cumulonimbus cloud played the roles of the accumulation of water vapor transported by the valley wind, the formation of rain from the water vapor and the precipitation to the surface. Furthermore, it is considered that the outflow from the cumulonimbus cloud played the roles not only of the formation of new horizontal convergence with the valley wind on the downslope side, but also the re-transportation of water vapor to the peak of the mountains.

Acknowledgment: The GPS data was analyzed by the Meteorological Research Institute of JMA with use of the GIPSY/OASIS II software package developed by JPL/NASA.

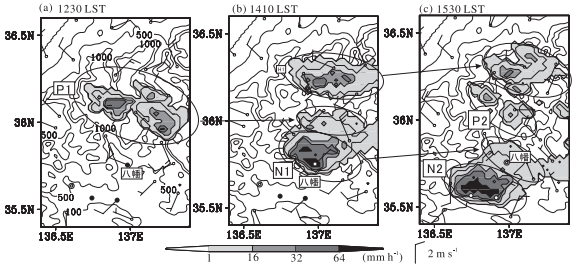

Fig. 8 The distribution of radar echo observed by JMA radar and the direction and speed of wind at each AMeDAS observation point at (a) 1230 LST (b) 1410 LST (c) 1530 LST. Black contours with shades are radar echo at 1, 4, 16, 32 and 64 mm h^{-1}. Barbs are the direction and speed of winds. Thin black contours indicate the terrain at 100, 500, 800, 1000, 1500, 2000, 2500 m ASL.

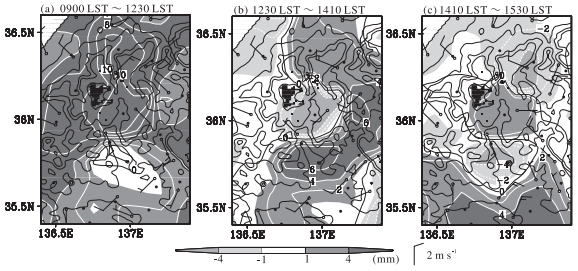

Fig. 9 The time deviation of PWV and the direction and speed of wind at each AMeDAS observation point at (a) 0900 LST – 1230 LST (b) 1230 LST – 1410 LST (c) 1410 LST – 1530 LST. White contours with shades are the time deviation of PWV every 2 mm. Barbs are the direction and speed of winds. Thin black contours indicate the terrain at 100, 500, 800, 1000, 1500, 2000, 2500 m ASL. Black shaded areas are the terrain over 1500 m ASL.

Characteristics of vertical circulation in the convective boundary layer over the Huaihe River Basin in China during early summer in 2004

A purpose of this study is to clarify the characteristics of the convective boundary layer (CBL) and vertical circulation in the CBL over the Huaihe River Basin during early summer in 2004. The Huaihe River Basin has a large plain in which farmland is nearly uniform and flat, and double cropping (wheat and rice) is cultivated annually. In early summer, the vegetation changes from mature wheat fields to paddy fields.

First, the data observed by 1290 MHz wind profiler radar (WPR) and 30 m flux tower were analyzed. In the former period in which vegetation was mature wheat fields or bare fields, the sensible heat flux (SHF) from the land surface was nearly equal to latent heat flux (LHF). In the latter period in which vegetation changed to paddy fields, LHF was much larger than SHF. The former period is defined as the "dry-case" and the latter period as "wet-case", and two fine days were selected for analysis. For the dry-case, a deep CBL corresponding to large SHF developed rapidly from early morning and thermal updrafts in the CBL were strong. For the wet-case, a shallow CBL corresponding to small SHF developed slowly from late morning and thermal updrafts in the CBL were weak. The circulation formed by thermal updrafts and inter-thermal downdrafts was detected only below the height of the CBL top, therefore the circulation in the dry-case was higher than that in the wet-case.

Next, numerical simulation using the CReSS (Cloud Resolving Storm Simulator) was conducted in order to investigate the three-dimensional structure including temperature and humidity, and to evaluate the vertical flux caused by the circulation. The surface heat flux and the development of the CBL on both cases were reproduced adequately. Vertical heat and moisture fluxes in the CBL were estimated (Fig. 10). In addition, contribution to buoyancy flux of these fluxes was evaluated. For the dry-case (Fig. 10a), the heat flux contributes nearly all of the buoyancy flux. As for the wet-case (Fig. 10b), in contrast, the contribution of the moisture flux was equal to that of the heat flux. Large contribution of the moisture flux to the buoyancy flux is characteristic of the CBL in humid continental areas.

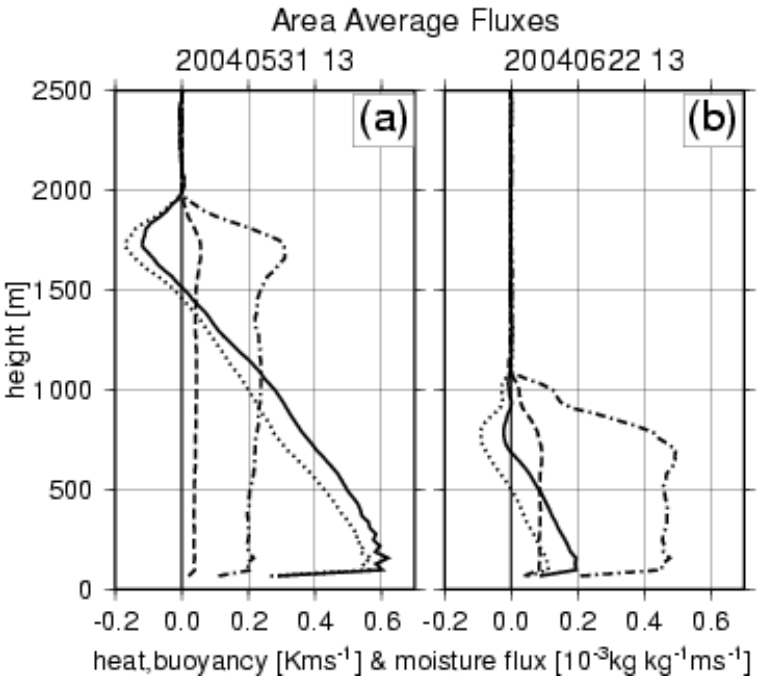

Fig. 10 Profiles of the vertical fluxes at 5 hours from the start of the simulation of the dry-case (a) and wet-case (b). The solid line indicates the buoyancy flux. The dotted line indicates the heat flux (contribution to the buoyancy flux). The dash-dotted line indicates moisture flux. The broken line indicates the contribution of the moisture flux to the buoyancy flux. The units of the moisture flux are [10^{-3} kg kg^{-1} m s^{-1}], those of others are [K m s^{-1}].

Numerical simulation of convective circulation in the atmospheric boundary layer over the Pacific Ocean under a subtropical high

In order to confirm the structure of convective circulation in the atmospheric boundary layer (ABL) over the western Pacific Ocean around the Southwest Islands of Japan under a subtropical high, we performed an intensive observation using radiosonde and Aerosonde in August 2002. From the Aerosonde observations a negative-correlation type eddy was appeared; that is, positive (negative) potential temperature and negative (positive) mixing ratio of water vapor anomalies exist simultaneously, even in the lower subcloud layer below the height of 0.2 km.

We examined the negative correlation type eddy observed by the Aerosonde in the lower subcloud layer by using the CReSS (Cloud resolving Strom Simulator) with a horizontal grid resolution of 100 m in order to resolve thermals in the subcloud layer. The horizontal domain of this 3-dimensional simulation is 10~10 km^2. We carried out numerical simulation by using the vertical profile observed by the radiosonde observation at 00 UTC on August 24, 2002, as the initial conditions.

Some thermals recognized by updraft regions develop in the subcloud layer in this simulation (Fig. 11). The horizontal scale of the thermals is about 0.5 to 1.5 km, and maximum vertical velocity in the thermals exceeds 1.5 m s^{-1}. A cool and moist air mass appears in the updraft regions not only in the upper subcloud layer but also in the lower one. Figure 12 shows vertical profiles of buoyant, heat and moisture fluxes, and the contribution of heat and moisture to the buoyant flux. A positive buoyant flux appears in the lower subcloud layer, therefore, thermals in this layer are driven by the positive buoyancy flux. This positive buoyant flux is driven by the contribution of moisture, not that of heat. This positive buoyant flux contributed by moisture is attributed to the small density of water vapor in comparison to the dry air. This should be attributed to the supply of small sensible and abundant latent heat fluxes from the sea surface under small air-sea temperature differences. We believe that the convective circulation driven by moisture should be considered a robust process of the convective circulation over the warm ocean: that is, over the subtropical and tropical western Pacific Ocean.

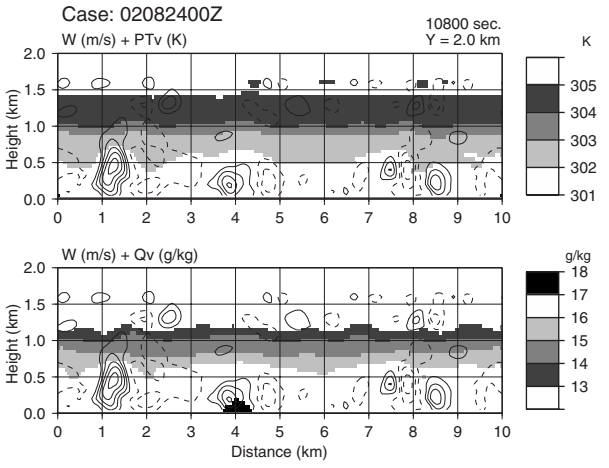

Fig. 11 Vertical cross sections of potential temperature (a), and mixing ratio of water vapor (b), with vertical velocity (contour) 3 hours from the start of the simulation. Contours for the updraft (solid line) and downdraft (broken line) are every 0.2 m s^{-1}.

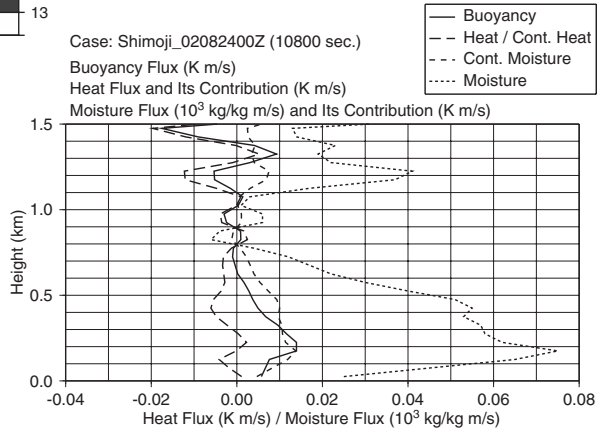

Fig. 12 Vertical profiles of buoyant flux (solid line), heat flux (long dashed line) and moisture flux (dotted line) 3 hours from the start of the simulation. The vertical profile of the contribution of heat to the buoyant flux is nearly equal to that of heat flux. The vertical profile of the contribution of moisture to the buoyant flux is shown by "short dashed line."

Laboratory for Climate System Study

Importance of the role of diurnal cycles of convection and rainfall in the climate system

The diurnal cycle of rainfall and convection is a most remarkable meteorological feature, particularly in the tropics/subtropics and monsoon regions. Energy, water and momentum exchanges through the diurnal cycle between the earth surface, atmospheric boundary layer and free atmosphere play a crucial role in the global climate system. To understand these processes, it is necessary that high-resolution hydrometeorological data in time-space, e.g., TRMM (Tropical Rainfall Measuring Mission) data and comprehensive *in-situ* data from raingauge stations be analyzed.

In the climate system study laboratory, we are conducting an integrated study on the time-space characteristics of diurnal cycles of rainfall and convection in various areas of monsoon Asia based on satellite and *in-situ* observational data. Here, we introduce some or our new results from the Tibetan Plateau, a key region for Asian summer monsoon, and from Borneo Island in the tropical marine continent, a heat source center for the global climate system.

Characteristics of Diurnal Variations in Convection and Precipitation over the Southern Tibetan Plateau during Summer

This study examined characteristics of the diurnal cycle of convection and precipitation over the complex mountain-valley terrain on the southern Tibetan Plateau (TP) in summer. Special attention was given to the evolution between noon and midnight.

Figure 1a shows a latitude-time section for cloud-cover frequency (CCF) averaged between 88° to 92°E. The left-hand figure shows the surface altitude averaged over the same longitudes. Small values of CCF are observed over the TP from 9 to 12 LST. CCF increases after 13 LST over mountain ranges C and D, reaching a maximum at 17–18 LST over the summits. Subsequently, areas of high CCF move from the two mountain ranges and merge over valley B, remaining there between 19 and 06 LST. Relatively high values of CCF also persist until 06 LST over the bottom of valley. A similar evolution occurred in rainfall frequency derived from TRMM PR (Fig.1b). The afternoon convection over the mountain ranges suggests convergence induced by a local circulation (a valley wind). A possible trigger for nocturnal convection is low-level convergence of down-slope flow from mountain ranges C and D which could be caused by surface cooling. Additionally, moisture transport associated with a wind system flowing along the Brahmaputra to valley B may enhance convection.

The formation and development of convective-type clouds and phase differences in the diurnal cycle over the southern TP are strongly influenced by mountain-valley terrain. However, the effect of a plateau-scale diurnal circulation system cannot be neglected in a detailed description of the diurnal convective cycle. Further study is needed to reveal the interactions between plateau-scale and regional-scale circulation systems and how they influence the diurnal cycle of convection over the southern TP in summer.

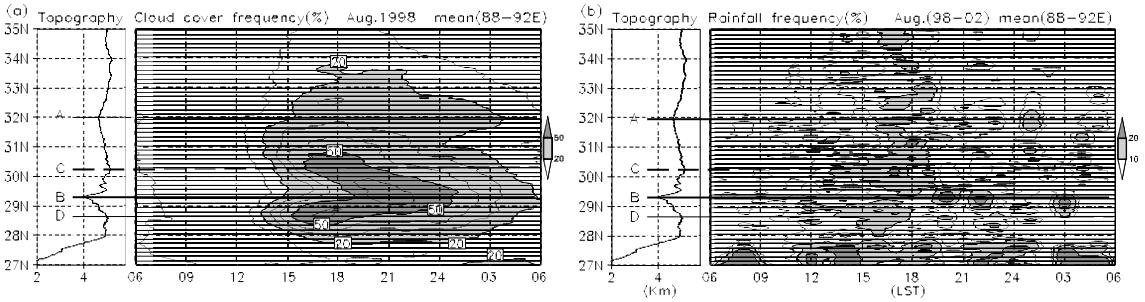

Fig. 1 (a) Latitude-Time section of cloud-cover frequency averaged between 88° and 92°E for August 1998. Contour interval is 10%. The left-hand figure shows surface altitude averaged over the same longitudes.
(b) The same as in (a) but for rainfall frequency averaged for five Augusts (1998–2002). The solid line denotes the 5% contour.

Time-space characteristics of rainfall over western Borneo Island

Rainfall variability has a large diurnal variation over Borneo Island. Using a density rainfall network over western Borneo, we investigated temporal and spatial characteristics of the diurnal cycle of rainfall. We used the daily rainfall data at 42 stations and the hourly rainfall data at 21 stations for 5 years from 1999 to 2003 in Sarawak.

The mean diurnal cycle of rainfall shows a remarkable difference in the rainfall peak times between the interior stations (at 18–22 LT) and the coastal stations (at 14–18 LT and 00–04 LT) in association with local and island-scale land-sea breezes.

To examine the temporal and spatial characteristics of rainfall variations, an empirical orthogonal function (EOF) analysis was applied to the daily rainfall averaged over five days running throughout this region. The eigenvector pattern of the first component shows positive values over the entire region. The time value of this component shows a dominant periodicity of about 30–60 days, which may be closely associated with the intraseasonal convective activity of the MJO time scale.

Additionally, the intraseasonal variability of rainfall more strongly influences the observations of the coastal rainfall stations in comparison with those of the interior rainfall stations. The occurrence of a midnight rainfall maximum at stations in the coastal area strongly depends on global-scale convection activity on an intraseasonal time scale. At night, land-sea breezes are likely to reinforce the low-level winds associated with intraseasonal variation. In the late evening, the rainfall maximum over the interior stations occurred around 1–3 LT hours later in the active phase of intraseasonal variability.

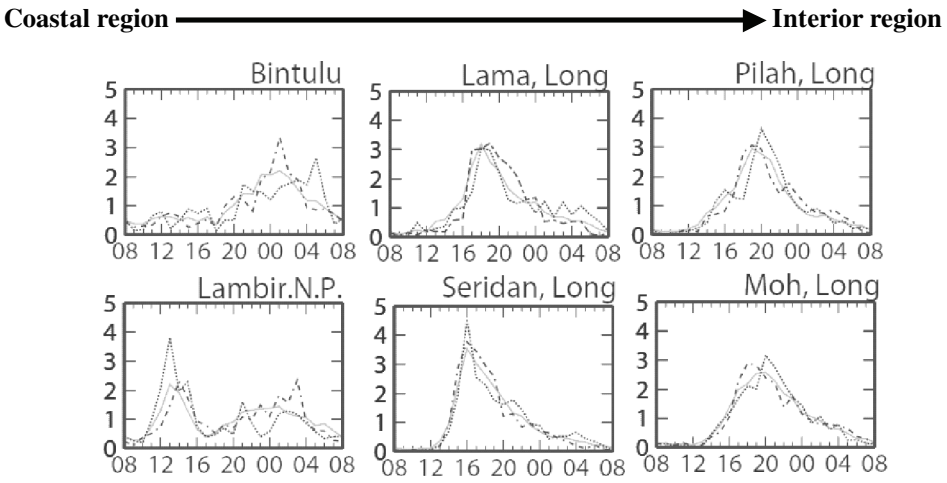

Fig. 2. Diurnal cycle of rainfall rates (mm h^{-1}) during the active (long dashed line), inactive (dashed line) phases of the MJO and 5-years mean (solid line).

Laboratory of Cloud Physics and Chemistry

Effects of Air Pollutants and their Air Mass on Aerosol Optical Properties over the East China Sea

The atmosphere over the East China Sea is often polluted by the inflow of air pollutants and covered by air masses from the continental regions of East Asia. The effects of air pollutants and their air mass on aerosol optical properties were studied near the East China Sea. Aerosol optical properties in the relatively marine atmosphere and anthropogenically polluted atmosphere were calculated applying two aerosol models (a homogenous mixture of aerosols and a core-shell mixture of aerosols). The size distribution of aerosol particles and atmospheric relative humidity (RH) measured aboard the aircraft (0 to 5 km in altitude) and the chemical composition of aerosol particles collected in Amami-Oshima Island were used in this study. Aerosol optical thickness was found to increase beyond a factor of 2 when under the influence of polluted air masses from continental regions. The results also showed that the effect of relative humidity on aerosol optical properties is significant when influenced by air masses from the Pacific Ocean, intermediate when influenced by anthropogenically polluted air masses, and low when influenced by anthropogenically polluted and dusty air masses. Overall, the study suggested that air pollutants and ambient relative humidity have strong effects on the increase of optical thickness under relatively marine and polluted atmospheric conditions, respectively.

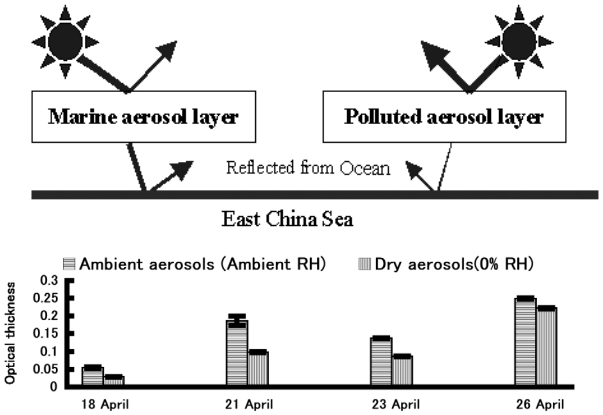

Fig. 1. Relationship between optical thickness and relative humidity in the relatively marine atmosphere and polluted atmosphere near the Amami-Oshima Island

Surface Observation of Atmospheric Gases, Aerosol Particles and CCN at Amami-Oshima Island

In order to examine the effect of air pollutants on microphysical and optical properties of lower clouds over the East China Sea, observation was conducted on atmospheric gases, aerosol particles and cloud condensation nuclei (CCN) at the northern end of Amami-Oshima Island during the periods of March to April, 2005 and October 2005 to January. 2006. In addition to surface observation, MODIS satellite data was analyzed to understand the microphysical and optical properties of lower clouds. The possibility was found that air pollutants from continental East Asia have a meso-scale change on the microphysical and optical properties of lower clouds.

Fig. 2. Observation car at Amami-Oshima Island

Effect of Air Pollutants on Microphysical Properties of Lower Clouds over the East China Sea by Aircraft Observation

Observational data showed that the concentrations of SO_2, aerosol particles and CCN were highly influenced by air pollutants transported from industrial areas in East Asia. CCN concentrations at 0.3% supersaturation (SS) were as high as 800 to 2000 cm^{-3} in the polluted maritime atmosphere. CCN concentration at different locations over the sea around the world is plotted in Figure 3. The concentration of CCN is remarkably higher over the East China Sea than that at any other location in the world. The results suggest that air pollutants from East Asia significantly increase CCN concentration and cloud droplet concentration over the East China Sea.

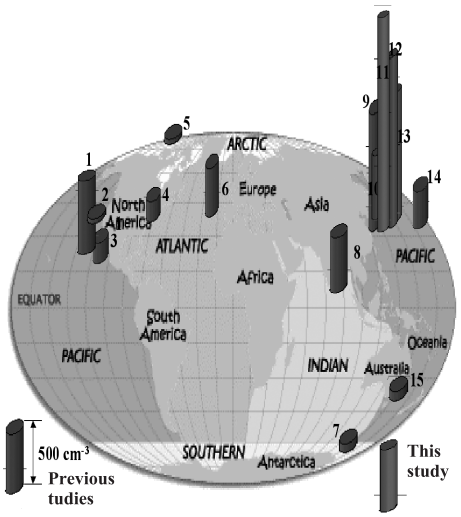

Fig. 3. Number concentration of CCN (0.3% SS) over the sea around the world. 1. Hudson and Xie (1999), 2. Hegg *et al.* (1991), 3. Berresheim *et al.* (1993), 4. Hudson and Xie (1999), 5. Hegg *et al.* (1995), 6. Harrison *et al.* (1996), 7. Hudson *et al.* (1998), 8. Hudson and Yum (2002), 9. Ishizaka *et al.* (1995), 10. Ishizaka and Adhikari (2003), 11. Adhikari *et al.* (2005, this study), 12. Adhikari *et al.*, (2003), 13. Ishizaka and Adhikari (2003), 14. Matsumoto *et al.* (1998) and 15 Gras (1987, 1989).

Microphysical properties of Clouds from Space Satellite Data

We estimated the microphysical properties of clouds (effective radius and optical thickness, etc.) using space satellite data to get useful information on the microphysical and optical properties of clouds and the influence of air pollutants on these properties over the East China Sea. The radiation brightness observed by the MODIS sensor on the Advanced Earth Observing Satellite Terra of NASA and NCEP/NCAR re-analysis data were analyzed using the algorithm by Dr. Takashi Nakashima of Tokai University. Figure 4(a) shows the relationship between the optical thickness of clouds and the optical effective radius of their cloud droplets over the sea near Amami-Oshima Island in the polluted atmosphere on March 18, 2005. On the other hand, Figure 4(b) shows the same relationship in the relatively marine atmosphere on March 22, 2005. It was suggested from the figures that the effective radius has a tendency to be smaller in polluted clouds than in relatively marine clouds and the optical thickness to be thicker in polluted clouds than in relatively marine clouds.

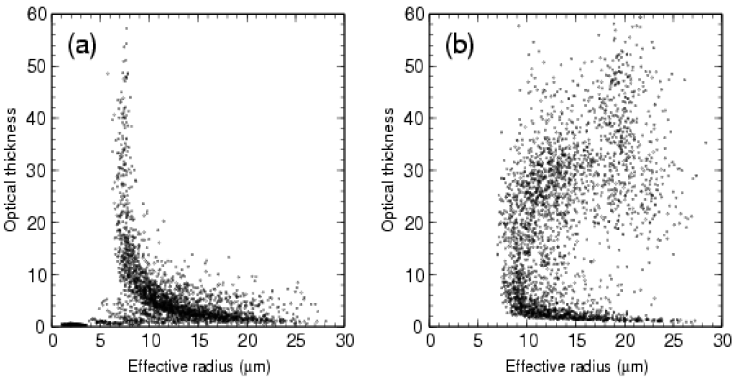

Fig. 4. Relationship between the optical thickness of clouds and the effective radius of their cloud droplets in an area of 300km × 300km near Amami-Oshima Island on March 18, 2005 (a) and March 22, 2005 (b).

Laboratory of Satellite Meteorology

Study on algorithm for a new generation space-borne precipitation radar

The Global Precipitation Measurement (GPM) is planned as the successor to the Tropical Rainfall Measuring Mission (TRMM). The core satellite of GPM will be equipped with a microwave radiometer (GMI) and dual-wavelength radar (DPR). The combination of DPR and GMI data may improve the retrieval of instantaneous precipitation rates. The main objective was to improve DPR precipitation retrieval using GMI data.

For liquid precipitation, a DPR algorithm without GMI data could be sufficient. However, wet snow retrieval could be very difficult since the variation of the signatures in DPR and GMI is very large. For dry snow, improvement may be possible using GMI data. The current combined algorithm is as follows:

(1) Estimate the snow particle diameter using the difference of the equivalent radar reflectivity on Ka and Ku-band radar channels.
(2) Make a forward calculation of the brightness temperature on the 85 GHz channel using DPR precipitation profiling using snow density as a parameter.
(3) Compare the calculated brightness temperature with GMI data.
(4) Determine the snow density to match the forward calculated and observed brightness temperatures.

To validate the algorithm, a three-dimensional precipitation structure with particle habit is essential. NICT Okinawa observatory should be the best site for the liquid precipitation observation site. Other instruments, such as 400 MHz/1.3 GHz windprofiler radars and disdrometers, are installed there. For the snow retrieval algorithms, Hokkaido University seems suitable. The Nagaoka site of the National Research Institute for Earth Science and Disaster Prevention could be an appropriate site for wet snow observation.

This work was supported by the Japan Aerospace Exploration Agency.

Atmospheric boundary layer observation over Okinawa Island using a C-band polarimetric Doppler radar

This observation was a continuation of observation from the prior fiscal year. From the previous observation, it was found that the C-band radar installed by the National Institute of Information and Communications Technology (NICT) has the capability to observe turbulent intensity and some large eddies in PBL. The continued observation was to gather more data on PBL development and was conducted for about two weeks in July, 2005. Intensive radio sonde launches (every two hours in daytime and three hours at night) and video camera sky watches were also performed. The observation covered weak rain cases (Fig. 1). A large eddy model simulation was also performed to reproduce the observational results.

This observation was conducted as part of LAPS project under CREST and also under the collaboration between HyARC and NICT.

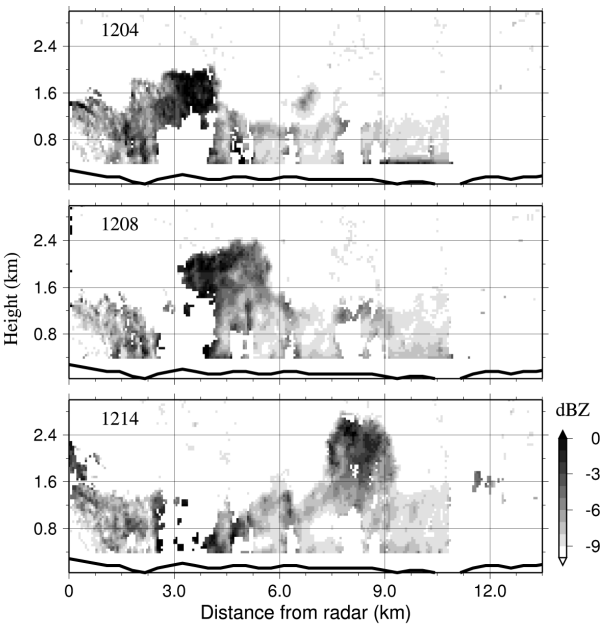

Fig. 1 Moist convection observed by the Doppler radar in Okinawa at 12 : 04 (upper), 12 : 08 (middle) and 12 : 14 (lower) on 8 July 2005. Abscissa is the horizontal range from the radar with a maximum of 14 km.

Heavy rain over the La Plata basin revealed by TRMM data

Global distribution of heavy rain frequency was produced using 6-year data of the Tropical Rainfall Measuring Mission (TRMM). The La Plata River basin was revealed to be a distinct region. The amount of annual precipitation is not so great, but the fraction of heavy rain (>30 mm/h) is very high. The heavy rains occur in the summer season, and are associated with a front which is generated by a collision of warm moist air and cold air due to a mid-latitude synoptic disturbances. A low-level moist air inflow from the Amazon region is essential for the rain. In winter, though low-level winds exist, the air is marginally moist and heavy rain is not induced. This mechanism may resemble the rains east of the Rocky Mountain range.

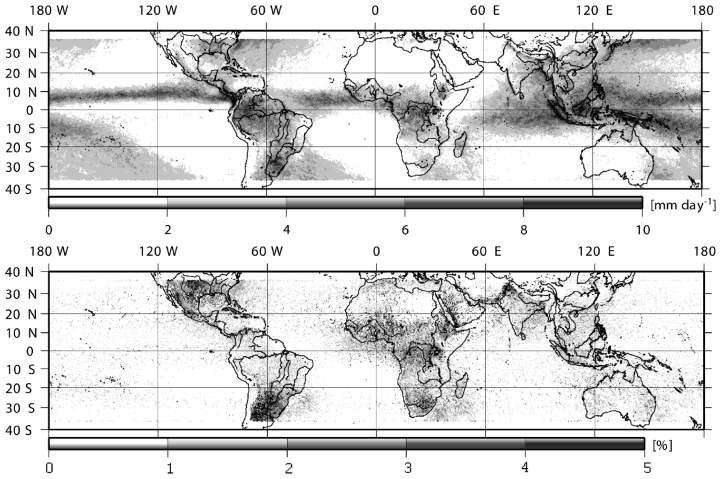

Fig. 2 Annual mean precipitation from six-year data (upper) and heavy rain (>30 mm/h) fraction of all rains (lower)

Diurnal variation of precipitation observed by space-borne sensors

The diurnal variations of precipitation and cloud systems over the tropic and mid-latitude regions were investigated using the Tropical Rainfall Measuring Mission (TRMM) data from 1998 to 2003 during June, July and August. The peak local time of minimum brightness temperature derived from the Visible and Infrared Scanner (VIRS) is compared with that of the maximum rain rate derived from the Precipitation Radar (PR) and the TRMM Microwave Radiometer (TMI). The peak time distributions are generally consistent with the TRMM combined product and previous studies. However, systematic peak time shifts appeared over land regions, particularly over western North America, the Tibetan Plateau, and oceanic regions such as the Gulf of Mexico. The peak time shift is in the order of PR, TMI, and VIRS with a few hours difference. The reason may be that the sensor signatures differ depending on the state of convective precipitation system evolution. PR directly detects the near surface rain. TMI mainly observes the deep convection with solid hydrometeors and retrieves strong rain in the mature stage. VIRS detects the deep convective clouds and anvils from mature to decaying state. The peak time shift particularly between PR (TMI) and VIRS is different depending on the regions.

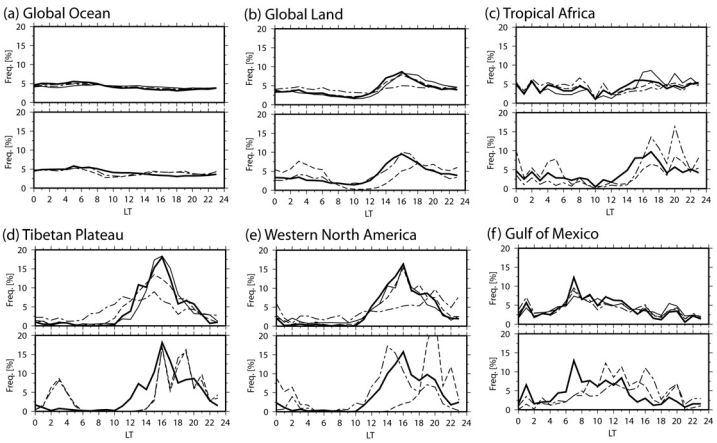

Fig. 3 Diurnal variation of the peak local time pixel's frequency of the maximum near surface rain rate (bold solid), storm height (thin solid), convective rain rate (dotted), stratiform rain rate (dash-dotted) derived from the PR2A24 data set (upper panels). Also surface rain rate from TMI (bold solid), minimum brightness temperature with (dash dotted) and without (dash) using split window technique (lower panels).

Laboratory of Eco-Hydrometeorology

Satellite-observed response of global terrestrial vegetation to climate variability

The inter-annual fluctuations in carbon sources and sinks or exchange fluxes between the atmosphere and biosphere are likely to be driven primarily by the effect of climate on ecosystem processes. Remotely sensed vegetation indices (the Normalized Difference Vegetation Index, NDVI) provide high spatial and temporal resolution coverage which allows monitoring of the dynamics of the global vegetation response to seasonal, inter-annual and episodic climate variability. This study aims to utilize monthly NOAA-AVHRR NDVI data over several years (1987–1997) to study the climatic and environmental factors governing the variability of vegetation growth and productivity on inter- and intra-annual time scales. An indirect and direct approach were followed. In the indirect approach, the decision tree algorithm for landcover classification was employed to generate 11-year landcover maps. The inter-annual variation in NPP was then estimated based on the annual variation in areas of healthy vegetation growth in the different biomes. Lag correlations between NPP and global annual anomalies of key climatic and environmental indicators were used to explain the observed variations. In the direct approach, trend analysis and multiple linear regression employing monthly NDVI as a proxy for aboveground net primary production (ANPP) were used to further investigate trends and variations in terrestrial biosphere productivity. Following the direct approach, this study also addressed the impact of large-scale weather variations driven by the two-fold ENSO cycle in the Equatorial Pacific. An attempt was made to better understand the timing and size of the impact of ENSO phases on vegetation production represented by NDVI by applying lag correlation analysis with Sea Surface Temperature (SST) and measures of standardized departures over the defined impact periods, respectively.

Consequently, the NPP estimates indicated that tropical and temperate forests are the most variable followed by deserts, while woodlands and grasslands exhibited only moderate variability. It has been found that the inter-annual variation in productivity of global vegetation is likely to influence the atmospheric CO_2 concentration across the same period. NDVI in all ecosystems exhibited an increasing trend over the investigated 11-year period (1987–1997) ranging between 0.7 and 1.9 (%/yr) allied with an analogous increase in precipitation (0.9–15%/yr).

The lag correlation indicated that the warm ENSO phases appear to have delayed (by 7 to 17 months) and has protracted negative impact on vegetation in all biomes related in most cases to a decrease in precipitation though rarely to an increase of temperature. This impact starts earlier in the tropical and subtropical regions but is delayed in the temperate and cold regions. Positive/negative impact of warm/cold ENSO phases on global vegetation are instantaneous and brief. Our results also indicate that ENSO has significant impact on boreal forests which were previously considered to have little or weak association with ENSO phases. In almost all biomes, warm ENSO phases tended to result in below average NDVI while cold and neutral phases tended to result in above average NDVI.

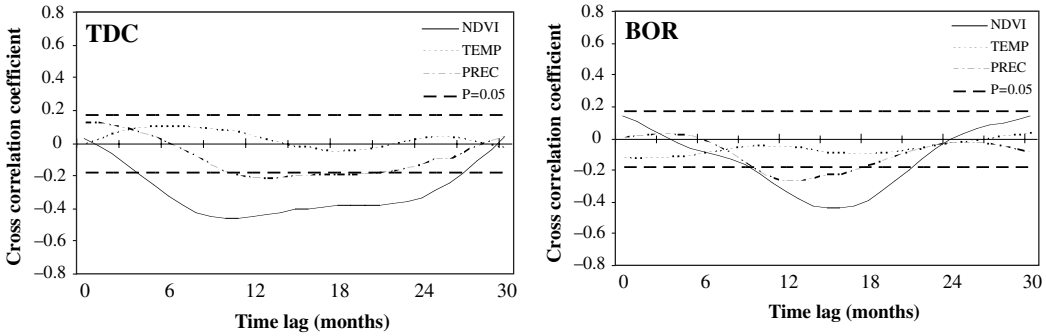

Fig. 1 Lagged correlation functions of monthly SST anomalies with monthly NDVI, temperature (TEMP) and precipitation (PREC) in tropical deciduous forests (TDC) and boreal forests (BOR). Correlations between bold dashed lines are statistically insignificant ($P > 0.05$). From the figures, it is clear that the time lag is larger in BOR than that in TDC, and that time lag of PREC shows similarity with the NDVI for each biome.

Seasonal variation in volatile organic compound (VOC) flux from a mixed forest

Emissions of biogenic volatile organic compounds (VOCs), which consist mainly isoprene and monoterpenes, are ten times as large as anthropogenic emissions. They are synthesized from carbons assimilated photosynthetically in plants and subsequently emitted. However, few measurements of VOC fluxes from temperate forests (for example, Japan) have been conducted. In this study, the VOC fluxes were measured using a relaxed eddy accumulation method in a deciduous and evergreen mixed forest located in Seto, Aichi, Japan from July to November 2005. According to the measurements, the fluxes of isoprene, α-pinene and β-pinene were -2.97–9.53 nmol m^{-2} s^{-1}, -0.17–0.61 nmol m^{-2} s^{-1}, and -0.50–0.27 nmol m^{-2} s^{-1}, respectively.

Compared with the gross primary production (GPP), which decreased gradually from summer to autumn, isoprene fluxes decreased rather rapidly. In many previous studies, isoprene emission rates exhibited a saturation behavior in relation to photosynthetically active radiation (PAR), not unlike the relationship between photosynthesis and PAR. In this study, however, while isoprene fluxes exhibited a positive relationship to PAR, there was no evidence of any saturation type behavior. Isoprene fluxes were affected by plant conditions following seasonal changes.

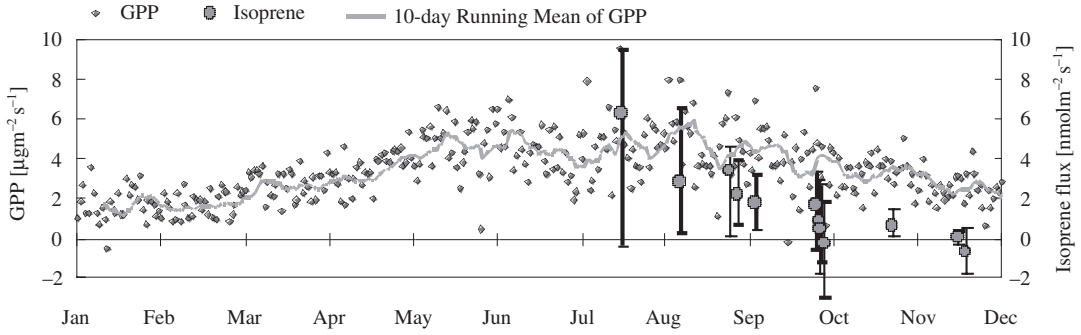

Fig. 2 Seasonal variations in gross primary production (GPP: left axis) and isoprene flux (Isoprene: right axis) observed in the mixed forest of Seto, Aichi, Japan. Also indicated are the 10-day running mean values of GPP (line), and each daily maximum/minimum range of isoprene flux.

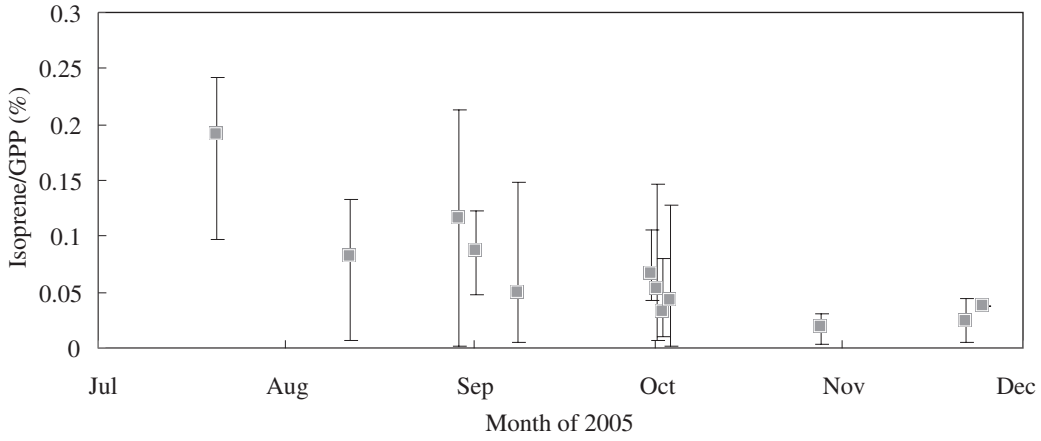

Fig. 3 Seasonal variation in daily ratio of isoprene flux to the GPP (Isoprene/GPP: %) for each observation day. Also shown is the daily maximum/minimum range of the ratio.

Laboratory of Ocean Climate Biology

The climate system surrounding us is governed by water and materials cycles in the hydrosphere and atmosphere of the earth. In this laboratory, we aim to study the interrelationship between climate change and ocean biogeochemistry on time scales ranging from a decade to century. The following is a brief description of our laboratory activities.

● Satellite Monitoring of Ocean Primary Productivity

Primary productivity is one of the key processes to understand the relationship between climate change and ocean biogeochemistry. A global view of the primary productivity can be attained by satellite remote sensing, but quantitative estimation of primary productivity is still hindered by the lack of validation data on temporally and spatially relevant scales. To fill this gap we developed, as a part of the Core Research for Evolutional Science and Technology (CREST) program during 1999–2004, an underwater profiling buoy system (POPPS – Project on Ocean Productivity Profiling System – Buoy) to measure *in situ* primary productivity. We are now trying to develop a practical monitoring system of ocean primary productivity by operating the profiling buoy system in combination with supporting data handling systems to merge satellite and *in situ* data. This is under a new 5-year continuation project as part of Solution Oriented Research for Science and Technology (SORST) started from 2004. The goal of the project is to design a practical monitoring system of global ocean primary productivity. The immediate task is to utilize satellite primary productivity data validated with the profiling buoy system for process studies on ocean biogeochemistry in response to physical forcings in order to demonstrate the usefulness of the validated satellite data.

Operational deployment and improvement of the underwater profiling buoy system

The underwater profiling buoy system is composed of an Underwater Winch System and a Profiling Buoy System. The system as developed has the capabilities of acoustic communication between the profiling buoy and the Underwater Winch System, and radio communication between the Profiling Buoy and the shore laboratory via cellular phone. The Profiling Buoy is equipped with sensors and normally stays at a depth ca. 150 m in calm and darkness, rising up for profiling measurements in the upper layers (to the surface) according to a pre-set schedule. Most of the measured data are processed in real time, and transmitted to the laboratory before the buoy sinks back to the resting position (at 150 m). At the observation station S3 in central Sagami Bay (ca. 1500 m of water depth), we successfully conducted operation of this system for 35 days during April and May, and for 14 days during July in 2005. The data transmission largely depends on sea, weather and radio wave conditions, but 35 data measurements out of a total of 66 were successfully transmitted during these observations (Fig. 1).

To extend operation of the buoy system to the open ocean, we tried deep-water mooring. To prepare for deep-water mooring, we made improvements on the buoy system such as making the profiling buoy more compact and installing iridium phones on the Underwater Winch System and the mooring line. The first deep-water mooring was attempted at the station off Shikoku (30°00'N, 135°32'E, ca. 4200 m of depth), in September and November 2005. Because of a first failure in September due to unexpected stretching of the mooring rope, we precisely measured every piece of the Vectran rope with a tension up to 400 kgN, and performed model simulation of the deployment depth of the Underwater Winch System. In the November deployment, the Underwater Winch System was placed within 10 m from the desired depth.

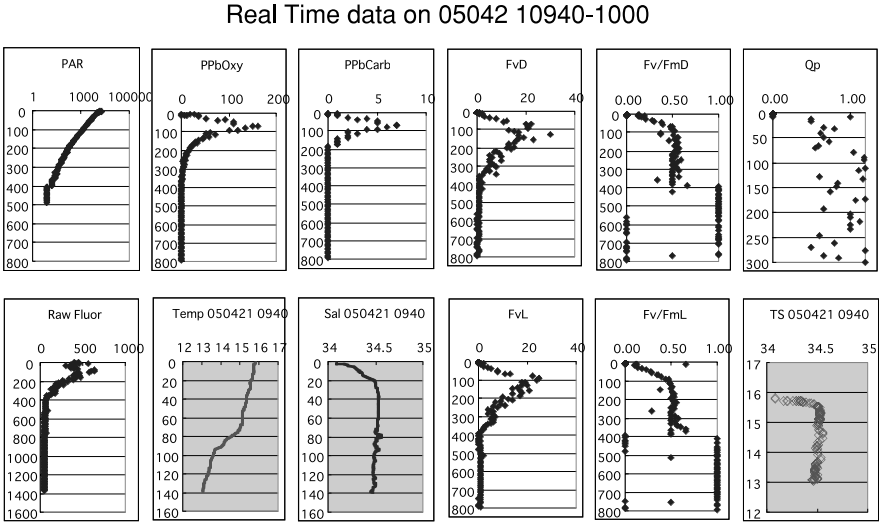

Fig. 1 Real-time data transmitted from the Underwater Profiling Buoy system in central Sagami Bay on 21 Apr., 2005. Measurements were conducted from 09 : 40 to 10 : 00. Shown from top left to right are figures for underwater photosynthetically available radiation (PAR), Chl *a* specific primary productivity (oxygen evolution), Chl *a* specific primary productivity (carbon assimilation), Variable fluorescence (in darkness), Quantum yield of photochemistry (in darkness) and photochemical quenching. Shown from bottom left to right are raw fluorescence, Temperature, Salinity, Variable fluorescence (in light), Quantum yield of photochemistry (in light) and T-S diagram. Data received as attached files to e-mail are automatically processed to calibrate/calculate and display/distribute products. Note that the depth scale is 10 fold.

Mooring-based fast repetition rate fluorometer (FRRF) for *in situ* observation of ocean primary production

FRRF can measure phytoplankton photosynthetic activity from a chlorophyll fluorescence transition in response to the exposure to a blue light flash with no experimental manipulation. In our project we developed a custom-made FRRF in collaboration with KIMOTO Electric Co., Ltd. as the main sensor of a POPPS buoy for real-time profiling measurements of the primary productivity. Here we report the FRRF measurements of the POPPS buoy system, which was moored at the S3 station in central Sagami Bay during the period from April 15 to May 10, 2005. During the observation period, Chl *a* concentration increased gradually from 27.9 to 188 mg m^{-2}, indicating the occurrence of a phytoplankton bloom (Fig. 2). Primary production increased with development of the phytoplankton bloom, and a maximum production of 40.9 mmolO_2 m^{-2} h^{-1} was found on May 8 when the Chl *a* concentration and irradiance were high. Using the mooring-based FRRF, we succeeded in measuring the primary production during the phytoplankton bloom, which is an unpredictable phenomenon in the ocean. This result demonstrates potential benefits of the POPPS buoy system for measurements of ocean primary production in high spatial and temporal resolution.

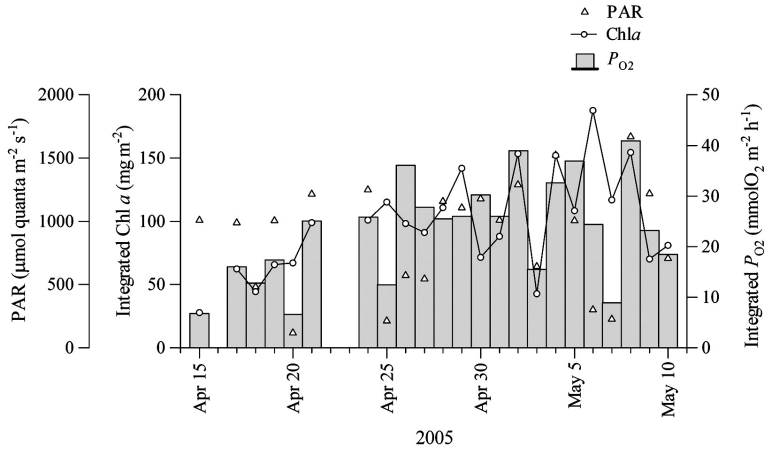

Fig. 2 Temporal variations in PAR, integrated Chl *a* and integrated primary production (P_{O2}) in central Sagami Bay.

Relationship between oxygen production and respiration in Sagami Bay

Algorithms for estimating ocean productivity with satellite data have been conventionally constructed based on measurements of net daily primary productivity. Therefore, the rate of algal respiration should be able to be determined when FRRF measurements of gross productivity are used for satellite data verification. To examine the relationship between gross production and respiration, the rates of gross and net oxygen production (GOP and NOP), and respiration in day and night time were measured during April, June and August 2004 at time-series station S3 in Sagami Bay. Light (day-time) respiration was found to be enhanced with a PAR between 19.6 to 46.3 mol Quanta m^{-2} d^{-1} whereas decreased at a PAR of less than 46.3 mol Quanta m^{-2} d^{-1} (Fig. 3). Significant algal respiration was observed that amounted to 28 to 37% of GOP. The NOP to GOP ratio varied from –0.11 to 0.79, whereas the GOP to daily respiration ratio ranged between 0.72 and 2.4. These ratios indicate that autotrophic and heterotrophic metabolisms in the study region were essentially in balance. The daily variability in NOP suggested that at saturated light intensities, the changes in NOP resulted due to the influence of light on respiration whereas at low light intensities, NOP varied due to the effect of light on GOP. Thus, the existence of net autotrophy or heterotrophy in the study region was dependent on light intensity through its effect on production/respiration ratios; therefore, our study suggests that the net heterotrophy is not a feature confined only to nutrient poor oligotrophic ecosystems.

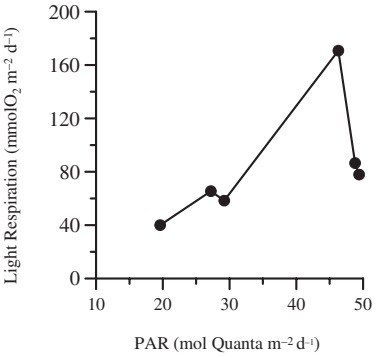

Fig. 3 Relationship of the day-time community respiration (Light respiration) and PAR.

Cell cycle of the *Synechococcus* population in the Sagami Bay

Picoplankton are important primary producers in marine environments, and their population dynamics are influenced strongly by cell cycles. In order to examine the relationship between diel variations in the picoplankton abundance and their cell division timing, natural populations of the most dominant picoplankton, *Synechococcus*, in Sagami Bay were sampled in June 2004, stained with DNA-specific fluorochrome SYBR Green I, and analyzed by flow cytometry. DNA histograms exhibited two peaks (G_1 and G_2 cells, containing one and two genome copies, respectively), separated by a trough of DNA-synthesizing cells (S cells). Within the mixed layer, the cells in G_1 phase entered the S phase soon after dawn and the fraction of cells in the S phase was high from 10:00 to 18:00. Below the mixed layer, the entry of the population into the S phase was delayed by 4 hours, and peaked at 14:00. The difference in the timings of the S phase could be attributed to the difference in light availability within the euphotic zone. Since the G_2 phase only lasts for a short period, the peak was not so obvious. The cell abundance within the mixed layer was found to peak after 4 to 6 hours from entry of the population into the S phase (Fig. 4). The decline in abundance even during the period when the fraction of cells in the S phase was at a maximum could be because of loss processes such as grazing pressure by the microzooplankton. These findings suggest that the population of *Synechococcus* divide at different times during the day depending on the light availability at the particular depth within the euphotic zone. Such a light dependence of picoplankton's cell division timing can control the diel variation in primary productivity in Sagami Bay.

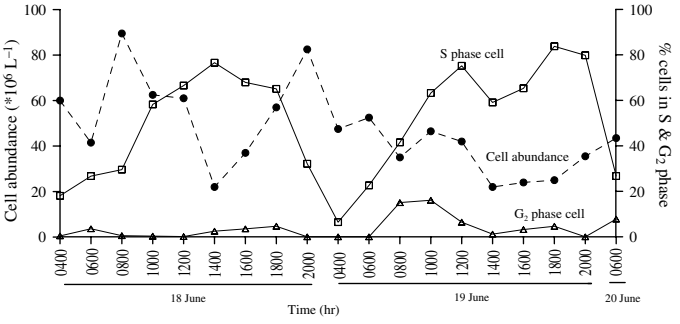

Fig. 4 *Synechococcus* cell abundance (●) and the percentage of cells in the S (□) and G_2 (△) phases of the cell cycle at a depth of 10 m in Sagami Bay.

Ultraviolet Radiation (UVR-C): A Potential Tool For The Control Of Optical Bio-fouling

As with any substratum immersed in seawater, sensors are susceptible to "Bio-fouling" which is caused by the adhesion of micro-organisms and macro-organisms, and can diminish sensor operation and performance. In order to achieve long-term monitoring of ocean productivity using the POPPS buoy system, the optical sensor windows of the FRRF must remain foul free during deployment. In this study we evaluated the effect of ultraviolet radiation (UVR-C: 254 nm) as an anti-fouling tool for FRRF. *In situ* anti-fouling experiments, in which glass test coupons were treated with different UVR conditions (exposure time and intensity), were carried out for 7 days in a dock basin of Kobe University where a high biomass is always found. The results showed the effect of UVR on marine biofouling to be significant in all UV treatments. The transmission spectra measurements revealed that the optical properties of the UVR-treated coupons, especially at higher UV treatments, did not change significantly in comparison to the non-treated coupons. Our results also revealed that the duration of the UVR exposure was found to be more critical to anti-fouling effectiveness than the intensity of UVR (Fig. 5), which could be related to the energy flux of the UV lamp as well as the timing of bio-fouling sequence/development of micro- and macro-fouling organisms. Altogether this study suggests the potential use of UVR as an anti-fouling tool, and opens up a new window for further exploration of UVR towards the development of bio-fouling control technology for optical sensors.

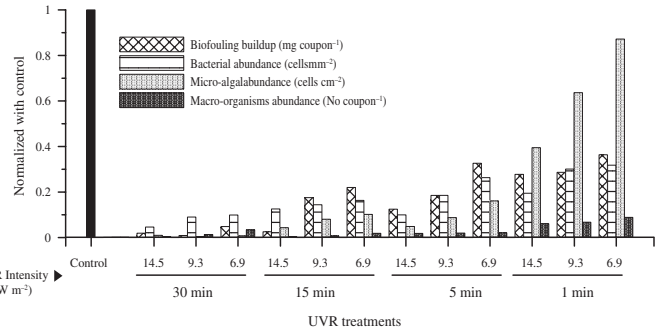

Fig. 5 Effect of ultraviolet radiation (exposure time: min h^{-1} and intensity: W m^{-2}) on bio-fouling buildup, bacterial, micro-algal and macro-organisms abundance.

Primary productivity in the upper Gulf of Thailand

In coastal seas relatively high primary production occurs due to the supply of land-driven nutrients, which accounts for about 1/5 to 1/3 of the global ocean production. The coastal primary productivity has large variability both in time and space in response to changes in environmental conditions caused by tidal movements, river inflow and human activities. Satellite remote sensing is expected to be a monitoring tool for such large variations, but an algorithm for estimating productivity has not been established for most highly eutrophic coastal regions. Here, in order to evaluate the relationship between primary productivity and underwater irradiance (PAR) in the upper Gulf of Thailand, we measured the Chl *a* specific photosynthetic rate (GP^B_C) using FRRF in winter and summer, Dec. 2003 (CU-2 cruise) and Jul. 2005 (CU-6 cruise) respectively. In both seasons, the Chl *a* distribution in the study area showed higher values in most inner Gulf areas where major rivers drained and lower values in the center of the Gulf. On the other hand, no obvious differences in the relationships between both profiles of GP^B_C and underwater PAR were found among regions within the upper Gulf and the seasons. As depicted in Fig. 6, GP^B_C exhibited maximal values (7~11 mgC mg Chl^{-1} h^{-1}) at around 300 μE m^{-2} s^{-1} of PAR and decreased values at PAR of less than 300 μE m^{-2} s^{-1}, which indicates that light inhibition always occurs at the surface layer. By using the P-E model of Platt *et al*. (1980) which includes the parameter of light inhibition effect, 91 to 94% of the variance in the observed GP^B_C can be simulated during both seasons. Additionally, the intensive FRRF measurements (2-hour intervals, 08 : 00–18 : 00) conducted in Nov. 2005 also showed a fixed P-E relationship, which is similar to those obtained from the CU-2 and CU-6 cruises. This implies that, regardless of habitat depth and season, phytoplankton photosynthesis throughout the upper Gulf responds to light availability in a similar fashion, which can be modeled by a simple, empirical P-E relationship. As a result, this study reveals that primary productivity in the upper Gulf is mainly light-controlled, and suggests that daily depth-integrated productivity can be estimated using our derived P-E equation and underwater PAR data. For this purpose, it is essential to use satellites to monitor/estimate the underwater photo-environments, that largely change in shallow coastal regions due to the input of land-driven materials and the resuspension of sediments by tidal currents.

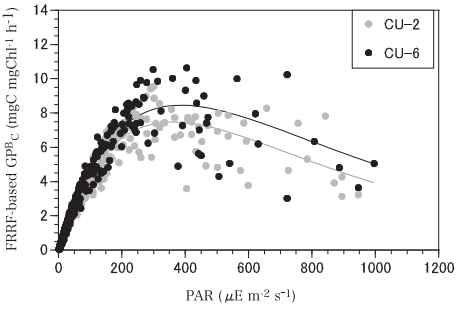

Fig. 6 Relationships between GP^B_C and underwater PAR in the upper Gulf of Thailand.

Laboratory of Bio-Physical Oceanography

Estimation of sea-surface currents in the eastern part of the East China Sea and the Japan Sea using both satellite altimetry data and ARGOS Buoy data

Enormous amounts of fresh water, heat, and materials are transported from the East China Sea (ECS) to the Japan Sea (JS) by the Tsushima Warm Current (TWC). Because the origin of the transported fresh water is the Changjiang River in China, concern is felt that the ocean environment in the JS as well as the ECS could experience drastic changes in the near future due to decreased river discharge after completion of the Three Goes Dam in the upper reaches of Changjiang. Therefore, an understanding of material transport in this area is important. However, the origin, current path, and variability of the TWC, which greatly influence material transport, are obscure. The aim of the present study is to evaluate both the overall mean sea-surface current and the monthly mean sea-surface currents in the eastern part of the ECS and the JS from 1995 to 2001, using satellite altimetry data and ARGOS Buoy data. Altimetry data provided velocity anomaly from the mean velocity during the data period, and absolute current velocities at a specific place and time are derived from the ARGOS Buoy. Therefore, if data from both sources at the same place and time can be obtained, calculating the mean sea-surface current during the satellite-altimetry data period from both data sources becomes possible, and consequently evaluation of the continuous current velocities that combined the mean sea-surface current with the anomalies also becomes possible. The mean sea-surface current from 1995 to 2001 evaluated by the method just described is shown in Figure 2. Branching from the Kuroshio in the ECS, the TWC along the Japanese coast, and the East Korea Warm Current, which is characterized by a northward strong current along the Korean Peninsula, are clearly seen. This is the first result to show the sea-surface current in the eastern part of the ECS and the JS based on observed data. Temporal and spatial variations of the sea-surface current in the eastern part of the ECS and the JS may be studied in the near future using the results of the present study.

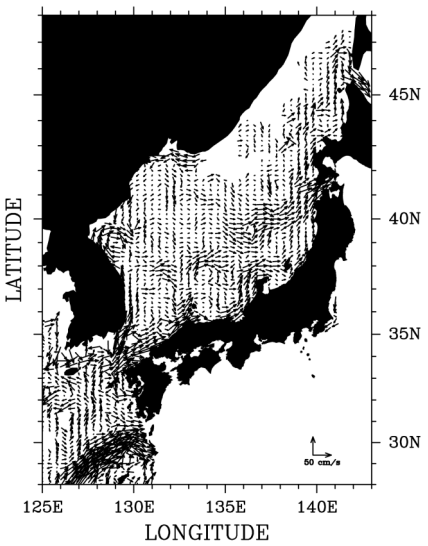

Fig. 1 Mean sea-surface current from 1995 to 2001, evaluated by altimetry data and ARGOS Buoy data

Summertime decrease in water temperature at the subsurface layer in Sagami Bay

Monthly CTD observation has been carried out at Station S3, which has been located in the central part of Sagami Bay since 2001. A decrease in water temperature around the subsurface layer in July and August has been noted. When this decrease water temperature takes place, concentrations of nutrients and chlorophyll *a* near the surface layer increase. This suggests that the phenomenon plays an important role in biological processes in Sagami Bay. However, the time and spatial scale of this phenomenon are uncertain. An objective of the present study is to reveal temporal and spatial variations in the summertime decrease in water temperature at the subsurface layer in Sagami Bay. Historical water-temperature data were interpolated in the grids, and the decrease in water temperature was evaluated by subtracting the water temperature for a given month from that for the previous month at all grids for different depths. The respective monthly average magnitudes of decrease in temperature in July, August, and September (for 1970–1997) at a water depth of 50 meters were 0.57°C, 1.34°C, and 1.23°C. The respective maximum average magnitudes of decrease in

temperature in July, August, and September (for each year from 1970–1997) at 50-meter water depth were 1.66°C (1971), 3.00°C (1977), and 4.89°C (1989). Because the Kuroshio flows off Sagami Bay, warm Kuroshio water sometimes enters the bay. Kuroshio variations are suspected of affecting the decrease in water temperature, but the correlation between the current path of the Kuroshio and the decrease in water temperature is not significant.

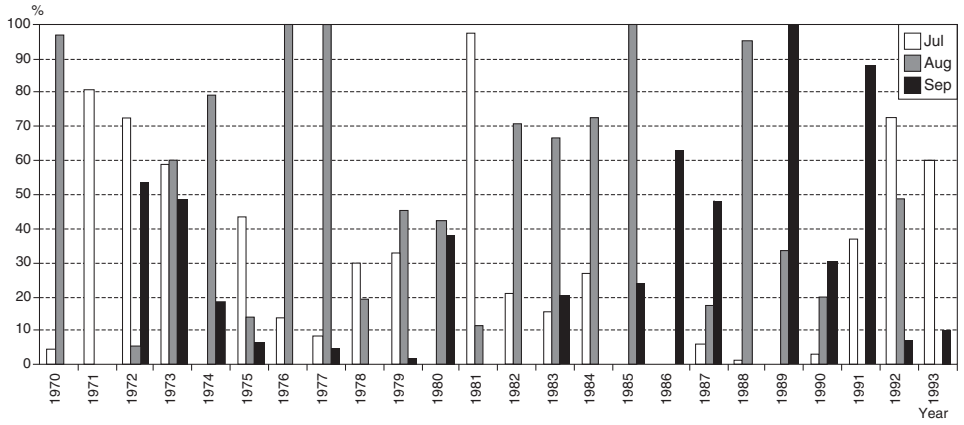

Fig. 2 Percentage of horizontal distribution in the summertime decrease of water temperature at 50-m depth in Sagami Bay

pCO_2 observations in the Tsushima Strait from spring to winter in 2005

Large amounts of river discharge from Changjiang affect environments in the East China Sea. A total of 70% of this fresh water is transported to the Japan Sea via the Tsushima Strait, and so variations in fresh-water inputs may affect the ecosystem structure and material cycles within the Japan Sea. The objective of this study is to reveal the effect of this fresh-water transport on the carbon cycle in this area from the measurements of partial pressure of CO_2 (pCO_2), water temperature, salinity, and chlorophyll *a* concentration (Chl*a*). Observations were conducted four times: twice in August, and once each in October and November 2005. The fresh-water transport is largest in August due to monsoon precipitation in China in the preceding months. The observation area is from the East Channel of the Tsushima Strait to the area off San'in. Seawater was pumped from the bottom of vessel at depths of 3 to 5 meters and at a flow rate of 50 L/min. to fill a 100-L container on the vessel. The pCO_2, surface water temperature (SST), salinity (SSS), and amount of Chl*a* inside the container were monitored continuously during each cruise. Water samples were collected for CO_2 system parameters, salinity, Chl*a*, and nutrients at intervals. The pCO_2 varied from 250 to 330 ppm in summer, which was on average 70 ppm lower than atmospheric pCO_2 (371 ppm). SST ranged from 26 to 28°C, and SSS ranged from 31 to 32 psu, which is highly diluted from an SSS of around 34.5 psu for typical seawater. The Chl*a* levels were lower than 0.3 mg/m^3. A negative correlation was found between SSS and Chl*a*, which indicates that Chl*a* increases in low-salinity water. The pCO_2 varied from 330 to 370 ppm in October, 20 ppm lower than atmospheric pCO_2 (375 ppm). SST varied from 23 to 27°C, and SSS ranged from 33 to 34 psu. This indicates that the waters had been cooled and became more saline than in the summer. The pCO_2 varied from 320 to 360 ppm in November, 40 ppm lower than the atmospheric pCO_2 (376 ppm). SST ranged from 16 to 22°C, and SSS ranged from 33.5 to 34.5 psu. The waters had become cooler and more saline than in October.

The pCO_2 was always lower than the atmospheric pCO_2 during the observations, indicating that this area acted as a sink for atmospheric CO_2. Further study is needed to analyze the vertical water-mass structure. Vertical profiles in salinity, temperature, Chl*a*, and pCO_2 were obtained on the transects which traverse the Tsushima Strait. Consideration must be given to the vertical water-mass structures, especially nutrient distributions, to reveal the mechanism which supports the high Chl*a* levels and low pCO_2 values in the less-saline water.

List of Publications

*: Staffs, students and research fellows in the HyARC.

1. Adhikari M.*, Y. Ishizaka*, H. Minda*, R. Kazaoka and J.B. Jensen
Vertical distribution of CCN concentration and their effect on microphysical properties of clouds over the sea near the Southwest Islands area in Japan. *Journal of the Geophysical Research*, VOL.**110**, D10203, doi: 10.1029/2004JD004758, 2005.
2. Babiker, I.S.*, A.A.M. Mohamed*, T. Hiyama* and K. Kato
A GIS-based DRASTIC model for assessing aquifer vulnerability in Kakamigahara Heights, Gifu Prefecture, central Japan. *Science of the Total Environment*, **345**, 127-140, 2005.
3. Bhatt, B.C.* and K. Nakamura*
Characteristics of Monsoon Rainfall around the Himalayas Revealed by TRMM Precipitation Radar. *Monthly Weather Review*, **133**, 149-165, 2005.
4. Chiba, S., Y. Hirota, S. Hasegawa and T. Saino*
North-south contrast in decadal scale variations in lower trophic level ecosystems in the Japan Sea. *Fisheries Oceanography*, **14**(6): 401-412, 2005.
5. Endo, N., B. Ai Li Kun and T. Yasunari*
Trends in Precipitation Amounts and the Number of Rainy Days and Heavy Rainfall Events during summer in China from 1961 to 2000. *Journal of the Meteorological Society of Japan*, 83-4, 621-631, 2005.
6. Fujinami, H.*, S. Nomura and T. Yasunari*
Characteristics of diurnal variations in convection and precipitation over the southern Tibetan Plateau during summer. *Scientific Online Letters on the Atmosphere (SOLA)*, **1**, 49-52, 2005.
7. Fukutomi, Y. and T. Yasunari*
Southerly Surges on the Submonthly Timescales over the Eastern Indian Ocean during the Southern Hemisphere Winter. *Monthly Weather Review*, **133**, no.6, 1637-1654, 2005.
8. Furuzawa, A.F.* and K. Nakamura*
Differences of rainfall estimates over land by Tropical Rainfall Measuring Mission (TRMM) Precipitation Radar and TRMM Microwave Imager (TMI) — Dependence on storm height. *Journal of Applied Meteorology*, **44**(3), 367-382, 2005.
9. Hashimoto, S., N. Horimoto, Y. Yamaguchi, T. Ishimaru and T. Saino*
Relationship between net and gross primary production in the Sagami Bay, Japan. *Limnology and Oceanography*, **50**(6), 2005.
10. Hirose, M. and K. Nakamura*
Spatial and diurnal variation of precipitation systems over Asia observed by TRMM Precipitation Radar. *J. Geophys. Res.*, **110**, D05106, doi: 10.1029/2004JD004815, 2005.
11. Hiyama, T.*, K. Kochi, N. Kobayashi* and S. Sirisampan
Seasonal variation in stomatal conductance and physiological factors observed in a secondary warm-temperate forest. *Ecological Research*, **20**, 333-346, 2005.
12. Islam, M.N, T. Terao, H. Uyeda*, T. Hayashi and K. Kikuchi
Spatial and Temporal Variations of Precipitation in and around Bangladesh. *Journal of the Meteorological Society of Japan*, **83**, 23-24, 2005.
13. Jingyang Chen, H. Uyeda*, Dong-In Lee and T. Kinosita
Establishment of Z-R relationships for the Baiu precipitation using the window probability matching method. *Meteorological Applications*, **12**, 207-215, doi: 10.1017/S1350482705001714, 2005.
14. Kajikawa, Y. and T. Yasunari*
Interannual valiability of the 10-25 and 30-60 day variation over the South China Sea. *Geophys. Res. Lett.*, **32**, L04710, doi: 10.1029/2004GL021836, 2005.
15. Kumagai, T., T. Saitoh, Y. Sato, H. Takahashi, O.J. Manfroi, T. Morooka, K. Kuraji, M. Suzuki, T. Yasunari* and H. Komatsu
Annual water balance and seasonality of evapotranspiration in a Bornean tropical rainforest. *Agricultural and Forest Meteorology*, **128**, 81-92, 2005.

16. Li, J. and K. Nakamura*
Vertical distribution of the mirror image returns observed by TRMM PR and estimated for a 35-GHz radar. *Journal of Atmospheric and Oceanic Technology*, **22**(11), 1829-1837, doi: 10.1175/JTECH1819.1, 2005.

17. Ma, Xieyao, T. Yasunari*, T. Ohata and Y. Fukushima
The influence of river ice on spring runoff in the Lena river, Siberia. *Annals of Glaciology*, **40**, 123-127, 2005.

18. Maki, M., K. Iwanami, R. Misumi, S.-G. Park, H. Moriwaki, K. Maruyama, I. Watabe, D.-I. Lee, M. Jang, H.-K. Kim, V. N. Bringi and H. Uyeda*
Semi-operational rainfall observations with X-band multi-parameter radar. *Atmospheric Sci. Letters*, **6**, 12-18, 2005.

19. Minda, H.* and K. Nakamura*
High temporal resolution path-average rain-gauge with 50 GHz band microwave. *Journal of Atmospheric and Oceanic Technology*, **22**(2), 165-179, 2005.

20. Ohigashi, T.* and K. Tsuboki*
Structure and Maintenance Process of Stationary Double Snowbands along the Coastal Region. *Journal of the Meteorological Society of Japan*, **83**, 331-349, 2005.

21. Saito, H., K. Suzuki, A. Hinuma*, T. Ota, K. Fukami, H. Kiyosawa, T. Saino* and A. Tsuda
Responses of microzooplankton to in situ iron fertilization in the western subarctic Pacific (SEEDS). *Progress in Oceanography*, **64**(2-4), 223-236, 2005.

22. Sarma, V.V.S.S.*, O. Abe, S. Hashimoto, A. Hinuma* and T. Saino*
Seasonal variations in triple oxygen isotopes and gross oxygen production in the Sagami Bay. *Limnology and Oceanography*, **50**(2), 544-552, 2005.

23. Shinoda, T.*, H. Uyeda* and K. Yoshimura
Structure of moist layer and sources ofwater over the southern region far from the Meiyu/Baiu front. *Journal of the Meteorological Society of Japan*, **83**, 137-152, 2005.

24. Shusse, Y., K. Tsuboki*, B. Geng, H. Minda* and T. Takeda
Structure and Evlution of Deeply Developed Convective Cells in a Long-Lived Cumulonimbus Cloud under a Weak Vertical Wind-Shear Condition. *Journal of the Meteorological Society of Japan*, **83**, 351-371, 2005.

25. Sukigara, C.* and T. Saino*
Temporal variations of δ^{13}C and δ^{15}N in organic particles collected by a sediment trap at a time-series station off the Tokyo Bay. *Continental Shelf Research*, **25**(14), 1749-1767, 2005.

26. Strunin, M.A. and T. Hiyama*
Spectral structure of small-scale turbulent and mesoscale fluxes in the atmospheric boundary layer over a thermally inhomogeneous land surface. *Boundary-Layer Meteorology*, **117**, 479-510, 2005.

27. Suzuki, K., A. Hinuma*, H. Saito, H. Kiyosawa, H. Liu, T. Saino* and A. Tsuda
Responses of phytoplankton and heterotrophic bacteria in the northwest subarctic Pacific to *in situ* iron fertilization as estimated by HPLC pigment analysis and flow cytometry. *Progress in Oceanography*, **64**(2-4), 167-187, 2005.

28. Tadokoro, K., S. Chiba, T. Ono, T. Midorikawa and T. Saino*
Interannual variations of Neocalanus copepods biomass in the Oyashio water, western subarctic North Pacific. *Fisheries Oceanography*, **14**(3), 210-220, doi: 10.1111/j. 1365-2419. 2005. 00333.x, 2005.

29. Wang, C.C., G.T.J. Chen, T.C. Chen and K. Tsuboki*
A numerical study on the effects of Taiwan topography on a line convection during the Mei-yu season. *Monthly Weather Review 133*, no.**11**, 3217-3242, 2005.

30. Zhao, C., Y. Ishizaka* and D. Peng
Numerical study on impacts of multi-component aerosols on marine cloud microphysical properties. *Journal of the Meteorological Society of Japan*, Vol.**83**, No.6, 977-986, 2005.

Hydrospheric Atmospheric Research Center (HyARC)

Nagoya University

Furo-cho, Chikusa-ku, Nagoya 464-8601, Japan

Office:

Telephone: +81-52-789-3466

Facsimile: +81-52-789-3436

Home Page: http://www.hyarc.nagoya-u.ac.jp/hyarc/

The 2005 Annual Report was published March 2007 by the Hydrospheric Atmospheric Research Center (HyARC) Nagoya University. Copies of this report are available from the office of the Center.

Printed by Nagoya University COOP


HyARC
Hydrospheric Atmospheric Research Center, Nagoya University